REPORT SNO 6799-2015

Current conditions in the Oslofjord
Focus on current strength along the bottom

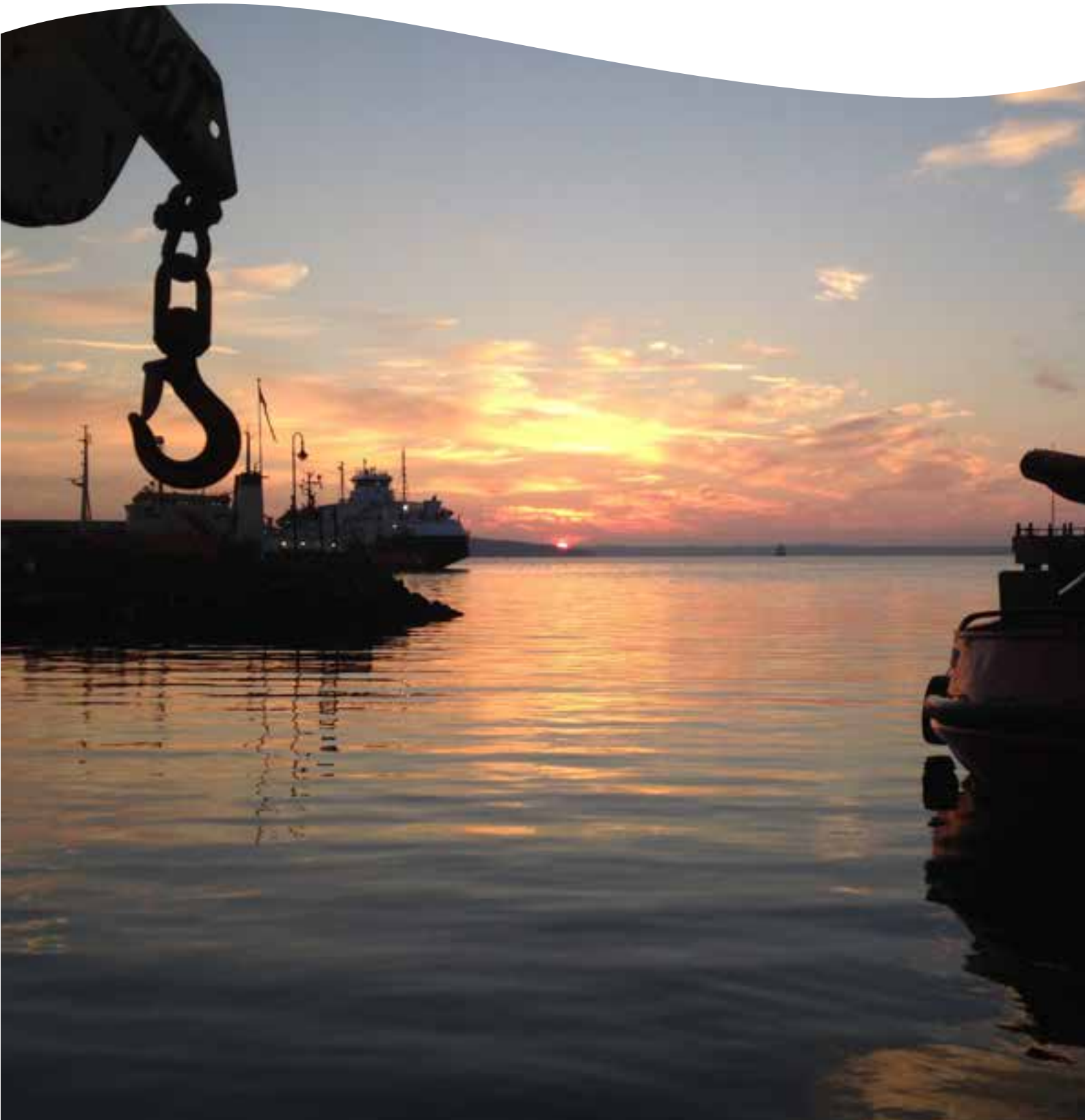

Norwegian Institute for Water Research
– an institute in the Environmental Research Alliance of Norway

REPORT

Main Office
Gaustadalléen 21
NO-0349 Oslo, Norway
Phone (47) 22 18 51 00
Telefax (47) 22 18 52 00
Internet: www.niva.no

NIVA Region South
Jon Lilletuns vei 3
NO-4879 Grimstad, Norway
Phone (47) 22 18 51 00
Telefax (47) 37 04 45 13

NIVA Region East
Sandvikaveien 59
NO-2312 Ottestad, Norway
Phone (47) 22 18 51 00
Telefax (47) 62 57 66 53

NIVA Region West
Thormøhlens gate 53 D
NO-5006 Bergen Norway
Phone (47) 22 18 51 00
Telefax (47) 55 31 22 14

Title	Report No..	Date
Current conditions in the Oslofjord Focus on current strength along the bottom	6799-2015	5.10.2015
	Project No. 14290	Pages 57
Author(s) André Staalstrøm (NIVA) Peygham Ghaffari (Akvaplan-niva)	Topic group Physical oceanography	Distribution Open
	Geographical area Oslofjord	Printed NIVA

Client(s)	Client ref.
Statnett	

Abstract

The objective of this project has been to assess how strong the current conditions near the bottom can be in extreme cases. Extreme value analysis has been applied to current observations near the bottom at six stations in the Oslofjord. The length of the observation period was up to seven weeks, from mid-September to the end of November 2014. The result from the extreme value analysis was multiplied with safety factor of 1.5 to account for possible additive effects of barotropic and baroclinic forcing. The strongest currents were found where the fjord is relatively narrow, in the Drøbak Sound. This was stations Filtvedt (Km1) and Brenntangen (Kn2), where the extreme value current with a return period of 50 years multiplied with the safety factor was 75 and 99 cm/s, respectively. A more realistic extreme value for these two stations is the result from the extreme value analysis with a return period of 10 years, which were 45 and 59 cm/s for the two stations respectively. The stronger current in the more narrow part of the fjord can be explained by a stronger tidal signal due to the fjord geometry. In both the two transects across the fjord, it was the shallowest stations that had the highest current velocities. This can be explained by the fact that the horizontal pressure gradient has a tendency to decrease with depth.

4 keywords, Norwegian	4 keywords, English
1. Oslofjorden	1. Oslofjord
2. Strømmålinger	2. Current measurements
3. Analyse for ekstreme verdier	3. Extreme value analysis
4. Fjorddynamikk	4. Fjord dynamics

André Staalstrøm
Project Manager

Lars Golmen
Quality control

Kai Sørensen
Research Manager

ISBN 978-82-577-6534-7

Current conditions in the Oslofjord

Focus on current strength along the bottom

Preface

This report is part of a research project where Statnett, NIVA, Akvaplan-niva and the University of Oslo participate, called CurOF. The main product of the project is this report and a master thesis in physical oceanography, that will be written on a later stage by Ole-Henrik Botvar, supervised by Professor Joseph Henry Lacasce. The observations of currents will also be used to validate a newly developed hydro dynamical model for the Oslofjord, called the FjordOs-model (www.fjordos.no).

All field work has been conducted from R/V Trygve Braarud, where the crew Sindre Holm, Jan Sundøy and Tom Opsahl have had the responsibility for safety during every step of the operation. Geir Olaf Jensen has been the main contact person at Statnett.

The analysis in this report is done by André Staalstrøm and Peygham Ghaffari. The master student Ole-Henrik Botvar has assisted during the field work.

Oslo, 17/8-2015

André Staalstrøm

Contents

Summary

The objective of this project has been to assess how strong the current conditions near the bottom can be in extreme cases in the Oslofjord.

Extreme value analysis has been applied to current observations near the bottom at six stations in the Oslofjord. Four of the stations was situated in a transect across the fjord just south of the island Bastøy and two stations was situated across the fjord in the southern part of the Drøbak Sound. The length of the observation period was up to seven weeks, from mid-September to the end of November 2014.

A safety factor of 1.5 was estimated based on comparison between the maximum observed sea level amplitude during the measurement period and maximum observed sea level amplitude for the period 2000-2013. The result from the extreme value analysis was multiplied with this factor to account for possible additive effects of barotropic and baroclinic forcing.

The strongest currents were observed and the most extreme values were estimated at the stations where the fjord is relatively narrow, in the Drøbak Sound. This was stations Filtvedt (Km1) and Brenntangen (Kn2), where the extreme value current with a return period of 50 years multiplied with the safety factor was 75 and 99 cm/s, respectively. The probability for these extreme current values to appear is very small, since the extreme value with a return period of 50 years must occur at the same time as an extreme storm surge event. A more realistic extreme value for these two stations is the result from the extreme value analysis with a return period of 10 years, which were 45 and 59 cm/s for the two stations respectively.

The stronger current in the more narrow part of the fjord can be explained by a stronger tidal signal due to the fjord geometry. In both the two transects across the fjord, it was the shallowest stations that had the highest current velocities. This can be explained by the fact that the horizontal pressure gradient has a tendency to decrease with depth.

1. Introduction

1.1 Background

Norway has a complicated coastline characterized by numerous fjords stretching far inland. It is often necessary to cross these fjords to build infrastructure, such as bridges or cables. Considering the dimensioning of structures to be placed in the sea and general safety, it is of interest to know how powerful the current conditions in the fjords can be.

There exist relatively few measurements of currents in the Oslofjord (**Figure 1**). There is a need for significantly more observations to understand how the current conditions can vary throughout the year and in different depths in fjords in general and in the Oslofjord in particular. In this project we want to contribute to fill this gap in knowledge. The main objective of this report is to assess how strong the currents along the bottom can be.

1.2 The Oslofjord

The Oslofjord stretches from the Swedish border and over to approximately Larvik in the south and northward to Drammen and Oslo. The topography of the fjord is thoroughly described be Baalsrud and Magnusson (1990). The whole fjord system has a surface area of approximately 1644 km^2. The fjord has two distinct sill fjords, the Drammensfjord and the Inner Oslofjord (that consist of the Vestfjord and the Bunnefjord), divided from the Outer Oslofjord with the sills at Svelvik and Drøbak. The outer Oslofjord has a surface area of approximately 1405 km^2 and a volume of approximately 103 km^3. The mean depth of the Outer Oslofjord is 70 m.

The sill depth between Skagerrak and the Outer Oslofjord is about 125 m, and the sill is covering a wide area and consists of a plateau between Koster and Larvik. Hvalerdypet with a maximum depth of 465 m is located inside this sill. The next sill is between Hvalerdypet and the Rauer Basin. Most of this sill area is areas with water depth of about 50 m, with a few narrow channels that cut through with depths down to 125 m. The Rauer Basin is divided from the Bastøy Basin with a sill depth of 205 m and the Bastøy Basin is divided from the Breiangen Basin and the Drøbak Basin with a sill area of about 100 m depths.

1.3 What are the driving forces for the currents?

It may be different driving forces behind the current conditions in a fjord. The tide is often the most dominant driving force where the fjord is narrow. When the water level fluctuates up and down with a period of approximately 12 hours, a large amount of water is pumped in and out of the fjord, and this sets up currents from the surface down to the bottom. The strength of the tidal current depends on whether the effect of the moon and the sun coincides (spring tide) or not (neap tide). Besides this, the tidal variation pattern is constant over time.

The current conditions can however be significantly enhanced by meteorological effects. An example of this is if a strong low pressure system passes over the fjord. The water level will rise as the low pressure system passes. This is called a storm surge event and strength of the current in the fjord may in such cases be several times stronger than the ordinary tidal current.

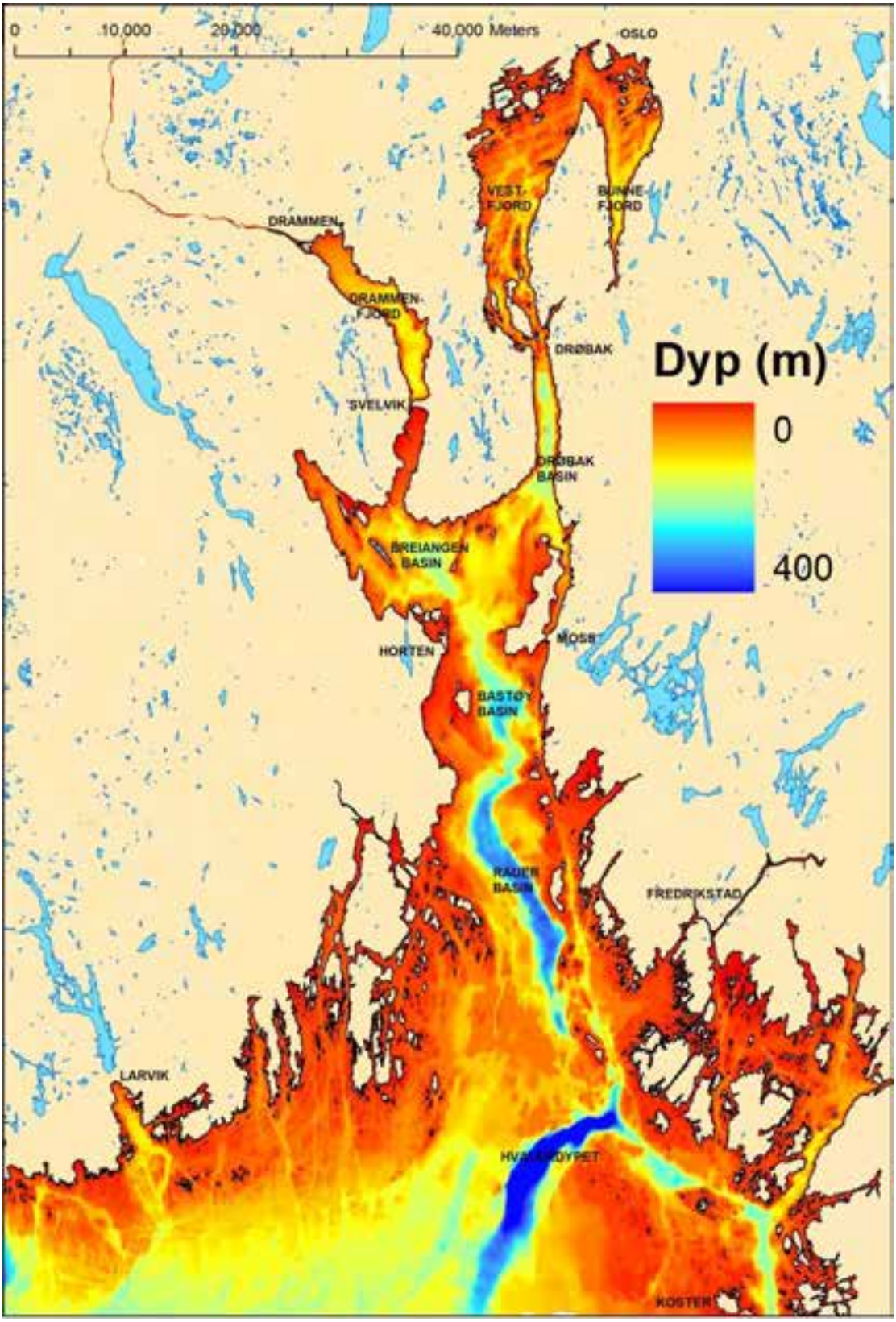

Figure 1. The bathymetry of the Oslofjord is shown with a colour scale where red indicate shallow areas and blue deep areas.

In addition to this, the currents can vary with different depths, if water masses of different density enter the fjord from the open ocean. All water movement is fundamentally caused by pressure differences. The tidal surface wave sets up a pressure force that has effect all the way from the surface down to the bottom, which causes the tidal flow. However, there will also be pressure forces which vary with depth, when water masses of different density are located in the same depth. This may cause significant currents without this being reflected as a change in the water level. These flow phenomena are therefore much more difficult to study because it requires observations at different depths.

Figure 2 shows the observed salinity in august 1988 measured from Skagerrak and into the Outer Oslofjord all the way to the Drøbak Sill. The sloping surfaces of constant salinity in Skagerrak are a typical characteristic of the coastal current (e.g. Aas, 1994). The path of the prevailing coastal current in Skagerrak follows the Swedish coastline and describes a loop and further follows the Norwegian coastline south-westward (e.g., Sætre, 2007, Røed & Fossum, 2003). This current system holds the more saline and heavy water in Skagerrak outside the Outer Oslofjord in place. In periods when this current system is weaker, this heavier water mass will penetrate into the Oslofjord, and cause variability in the observed currents for example just south of Bastøy. How often water from Skagerrak penetrates into the Oslofjord is not well established.

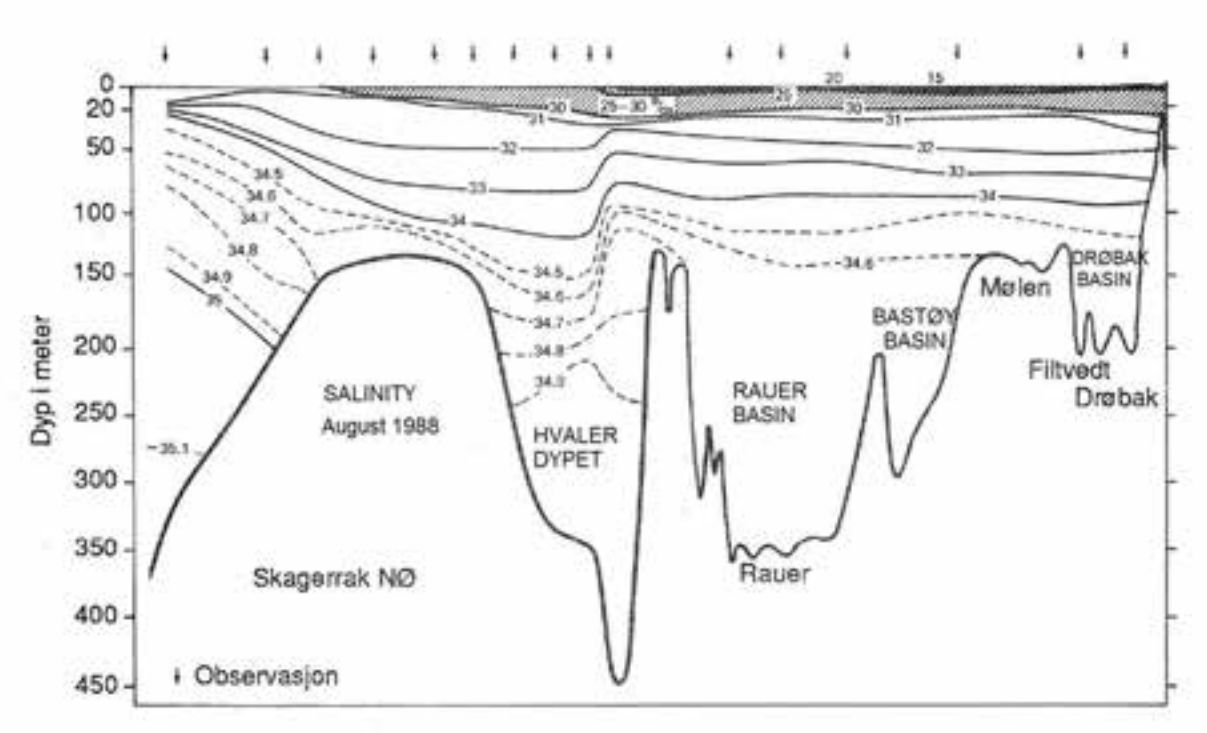

Figure 2. Salinity shown along a transect from the open ocean (Skagerrak) and into the Oslofjord. Surfaces of constant salinity are shown. The thick black line indicates the bathymetry. The figure is taken from Baalsrud and Magnusson (1990).

2. Methods

2.1 Current field variability

Variability in the current field caused by horizontal pressure gradients that vary with depth, will in this report be referred to as mean baroclinic flow. The term ”mean” is used because it is not associated with tidal variability, and the duration of such events is typically days, as in contrast to ”tidal” variability with variations with the common tidal periods (M_2, 12.42 hours, S_2, 12 hours etc.). Here it must be pointed out that non-tidal baroclinic flow also can occur with duration of only a few hours, but then in a more irregular pattern.

The term ”baroclinic” is used because the flow is caused by horizontal pressure gradients that vary with depth, as in contrast to the term ”barotropic” that refer to horizontal pressure gradients that do not vary with depth. Note that fresh water from rivers and direct wind stress also cause baroclinic flow, that is currents that vary with depth. Baroclinic flow caused by rivers can be referred to as estuarine circulation, where fresh water normally flows seaward near the surface, and an opposite directed current is located deeper in the water mass that compensate for the water that the river water entrains on its way. Direct wind stress can cause flow more or less in the direction of the wind depending on the geometry of the fjord. This type of baroclinic flow is usually of relatively short duration, but is not associated with tidal periods. The direct wind stress has also an important indirect effect, since it cause the upper layer to be mixed and therefore create new water masses that potentially sets up new horizontal pressure gradients.

The meteorology also causes changes in the sea level, which create mean barotropic flow. If the effect of the weather causes a rise of the sea level, because the atmospheric pressure drops, this is called a storm surge event. This rather complex picture of what cause current variability, is organized in **Table 1**.

Table 1. Flow variability divided into four categories.

TIDAL BAROTROPIC FLOW Sea level change due to tides	MEAN BAROTROPIC FLOW Storm surge
TIDAL BAROCLINIC FLOW Internal tidal waves	MEAN BAROCLINIC FLOW Water masses Direct wind stress Estuarine circulation

To divide the observed variability of the current in a given direction at a given station, $u(z,t)$, is not a trivial task. The barotropic flow can be extracted by calculating the depth averaged mean, since this type of flow is caused by pressure gradients that not change with depth

$$u_0(t) = \frac{1}{H+\zeta}\int_{z=-H}^{z=\zeta} u(z,t)dz \quad (1)$$

where H is the mean water depth and ζ is the sea level. u_0 is sometimes called the depth integrated mode. The bathymetry make this picture more complex and the barotropic flow may change with depth where the slope in the sea bed is steep. Nevertheless the barotropic mode is assumed to be equal to the

depth integrated mode in much of the oceanographic literature. The baroclinic flow u_n can now be found by subtracting the barotropic flow from the observed current field, and the current can be divided into a part that varies with depth and a part that does not.

$$u(z,t) = u_0(t) + u_n(z,t) \tag{2}$$

Since the barotropic mode is associated with the sea level, it is sometimes referred to as the external mode. The baroclinic flow can be further divided into several internal modes, associated with internal waves.

Both the barotropic and the baroclinic flow, vary on different time scales. The tidal variability can be extracted by using harmonic analysis, where the observed currents are described by a sum of sine functions, with different amplitude, angular frequency and phase shift

$$\tilde{u}(z,t) = \sum_i U_i \sin(\omega_i t - \varphi_i) \tag{3}$$

To find the mean variability $\bar{u}$, a filter that remove oscillations with periods shorter than a given limit T . In this report we have used a limit of 25 hours. This is called a 25 hours low-pass filter.

Since the current caused by one driving force might affect the current caused by another driving force, it can be that the amplitude U_i of the tidal oscillation can change with different mean flow regimes, and it can be that the harmonic analysis (3) not captures all of the variability that takes place on tidal periods. Because of this, and also the fact that non-tidal oscillations with shorter periods than 25 hours always are present, a third component, u' , is necessary to describe all of the observed temporal variability.

$$u(z,t) = \bar{u}(z,t) + \tilde{u}(z,t) + u'(z,t) \tag{4}$$

2.2 Extreme value analysis (return period)

Extreme value theory is a powerful and yet robust framework to study the tail behaviour of a distribution. Embrechts et al. (1997) is a comprehensive source of the extreme value theory to the finance and insurance literature. Reiss and Thomas (1997) and Beirlant et al. (1996) also have extensive coverage on the extreme value theory. The extreme value theory has found large applicability in climatology, meteorology and recently in oceanography.

There are three mainstream available data sources for aforementioned geo-fluid studies: in-situ observation, remote sensing and atmospheric-oceanic models. Both type of the observations (in-situ and remotely) bare some measurement errors, and suffer from limited representativeness and are sporadic in space and time. On the other hand, the available models are depended on the observations in term of the validation and accuracy. Although, models can provide longer datasets, we still need observations to have accurate models. In addition, observations and models in operational scales are costly. The above-mentioned reasons justify the wide spreading application of the extreme value analysis in geo-fluid dynamics particularly when we need to study their hazardous aspects. In that connection, determining return periods based on relatively short times series for variable longer time frames has vital importance in coast effective engineering.

The normal distribution is the important limiting distribution for sample sums or averages as summarized in a central limit theorem. Similarly, the family of extreme value distributions is the one to study the limiting distributions of the sample maxima. This family can be presented under a single parameterization known as the generalized extreme value distribution (GEV). The theorem of Fisher and Tippett (1928) is in the core of the extreme value theory. The theory deals with the convergence of maxima. Suppose that $x_1, x_2, \dots, x_m$ is a sequence of independently and identically distributed random variables from an unknown distribution function $F(x)$ where $x \sim (\mu, \sigma_2)$ and m is the sample size. Denote the maximum of the first $n < m$ observations of x by $M_n = max(x_1, x_2, \dots, x_{mn})$. Given a sequence of $a_n > 0$ and b_n such that $(M_n - b_n)/a_n$, the sequence of normalized maxima converges in the following GEV distribution

$$H(x) = \begin{cases} e^{-(1+\xi\frac{x}{\beta})^{-1/\xi}} & if\ \xi \neq 0 \\ e^{-e^{-x/\beta}} & if\ \xi = 0, \end{cases} \quad (5)$$

Where $\beta > 0$ and x is such that $1 + \xi x > 0$ and ξ is the shape parameter (the tail index is defined as $\alpha = \xi^{-1}$). When $\xi > 0$, the distribution is known as the Frechet distribution and it has a fat tail. The larger the shape parameter, the more fat-tailed the distribution is. If $\xi < 0$, the distribution is known as the Weibull distribution. Finally, if $\xi = 0$, it is the Gumbel distribution. The Fisher-Tippett theorem suggests that the asymptotic distribution of the maxima belongs to one of the three distributions above, regardless of the original distribution of the observed data. Therefore, the tail behaviour of the data series can be estimated from one of these three distributions.

3. Field work

In the period from Monday 15th to Thursday 18th of September altogether seven rigs with instruments was deployed at seven positions in the Oslofjord. All but one rig had profiling current meters, while the last rig had TinyTag temperature loggers deployed at seven different depths between 20 and 120 m. At one station a single point current meter was deployed just below the profiling current meter. The research vessel F/F Trygve Braarud (from now on called TB) was used, and the deployment and recovery operation is described in detail in the operation plan (Holm, 2014). The following personnel participated during deployment and/or recovery:

Sindre Holm	TB captain
Tom Opsahl	TB crew
Jan Sundøy	TB crew
Geir Olaf Jensen	Statnett representative during deployment
Ole Petter Hobberstad	Statnett representative during recovery
André Staalstrøm	NIVA
Peygham Ghaffari	Akvaplan-niva
Ole-Henrik Botvar	University of Oslo (participated only during deployment)
Karina Hjelmervik	FjordOs project leader, observer (participated only during deployment)

In the period from Monday 24th to Wednesday 16th of November the seven rigs with instruments was recovered. During Monday 24th of November a safety briefing meeting was held on-board TB at Lysaker, where also Geir Olaf Jensen from Statnett participated. Changes in the Job Safety Analysis were communicated to everybody in the crew. All the instruments were recovered during Tuesday 25th of November, and demobilisation took place at Wednesday 26th of November.

Station positions were selected using a terrain model from the Statnett database. The positions for the instrument rigs are listed in Table 2 and shown in **Figure 3**. Note that station Km1 and Km2 was only 150 m apart, and is marked as one station in the map (Filtvedt). At one station (Laksetrappa) a single point current meter was deployed just below the profiling current meter. During the deployment and recovery and at to instances in between, profiles of temperature and salinity was measured with the Seabird CTD on-board TB at four stations listed in Table 3.

The six profiling current meters delivered good quality data during the measurement period from September 19th to November 25th, with a few exceptions. The exceptions were the Continental ADCP at Botnegrunnen where data recording was stopped at November 18th due to lack of memory in the instrument, and the Continental ADCP at Filtvedt where data recording was stopped at November 11th due to problems with the battery.

Below the instrument rig at each station is described.

Table 2. Target positions (WGS84) of the instrument rigs. Depths at the stations are from the Statnett terrain model.

Station	Name	Latitude	Longitude	UTM32 Easting	UTM32 Northing	Depth (m)	Instruments
Kp11.2 (Ri1)	Småskjær	59.350124	10.497661	585164.3	6579997.2	20	Aquadopp600 AQP1531 Transducer LRT2
Kp5.7 (Rl1)	Laksetrappa	59.343452	10.581023	589921.7	6579364.0	75	Aquadopp400 AQP4689 Transducer LRT3 Aanderaa Seaguard
Kp2.6 (Rm1)	Botnegrunnen	59.352375	10.626822	592502.0	6580420.1	96	Continental WAV6117 Transducer LRT4
Kp0.7 (Rn1)	Evje	59.363182	10.653576	593993.1	6581660.8	64	Aquadopp400 AQP2931 Transducer LRT5
Kn2	Brenntangen	59.581803	10.646087	592965.0	6605990.8	54	Aquadopp400 AQP5608 Transducer LRT6
Km1	Filtvedt Current meter	59.582064	10.627372	591907.5	6605993.8	153	Continental CNL6037 Transducer 207-2
Km2	Filtvedt Temperature	59.580778	10.626239	591847.0	6605849.0	125	7 TinyTags UIO1-7 Transducer 203-2

Table 3. CTD positions (WGS84). Parameters measured were depth (m), temperature (°C), salinity (PSU), fluorescence (mg/m³), turbidity (FTU) and sound velocity (m/s).

Station	Name	Latitude	Longitude	UTM32 Easting	UTM32 Northing	Depth (m)	Comments
OF-7b	Filtvedt	59.580717	10.633383	592251	6605852		New station defined south in the Drøbak sound
OF-5b	Tofteflaket	59.486450	10.540967	587275	6595232	128	New station defined in the western part of Breiangen
OF-4	Bastøy	59.359467	10.590233	590403	6581159		Station from the monitoring program
OF-3	Rauer	59.247000	10.610717	591870	6586666	350	Same as the sediment station H1

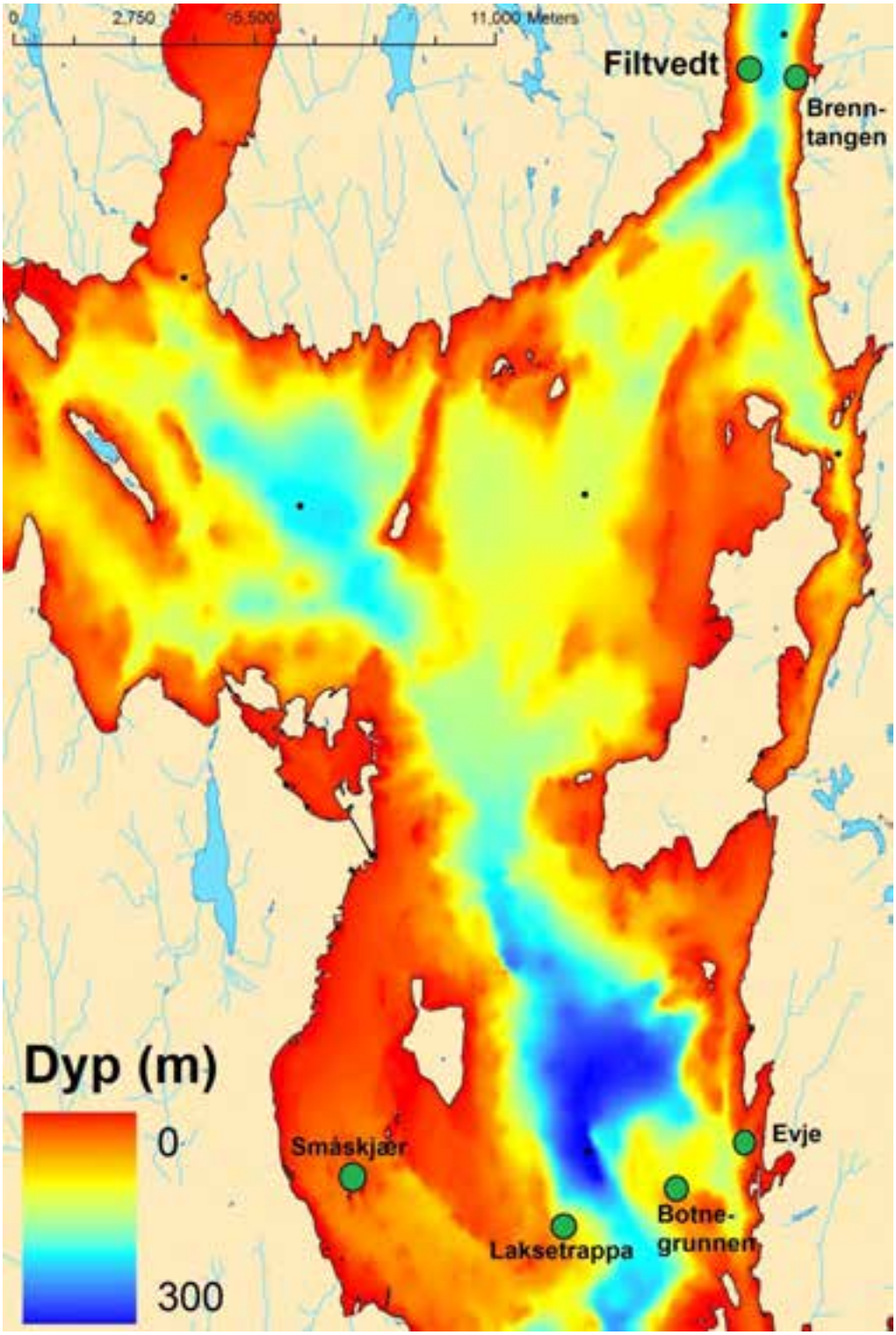

Figure 3. Map over the project area. The green dots show the positions of the current meter rigs.

3.1 Station Småskjær (Ri1)

The water depth at this station is 20 m. A Nortek Aquadopp 600 kHz was deployed approximately 2.2 m over the bottom. The instrument sends acoustic signals upward and into the water column along three beams oriented 25° from the vertical centre line. Particles in the water reflect the signal, and current speed along the beams is calculated based on the Doppler principle. The current vector is calculated using a tilt sensor and a magnetic compass. The frequency of 600 kHz gives limited vertical range, but allows for higher vertical resolution. A vertical resolution of 2 m was chosen. If the vertical resolution is increased, the precision of the measurements are decreased. The instrument gives a reading every 10 minutes, based on measurements during an averaging period. The averaging period was chosen to 180 seconds, giving a precision of 1.8 cm/s. A longer averaging period gives better precision, but then the instrument will use more battery. The power setting was set to the highest possible value (HIGH+). The background for this choice is that a lower power setting might give lower data quality if the water contains fewer particles.

Above the current meter two 28 cm diameter floats with a positive buoyancy of 8.4 kg each, was attached at the end of a 4 m long rope. The rig was weighted down with bio-bags containing approximately 90 kg of gravel. Between the bio-bags and the instrument a transponder with an acoustic release was mounted. The transponder had the identification number LRT2. The deployment of this instrument rig was finished September 16th 10:55 LT (**Figure 4**). Afterwards the position of the rig at the bottom was confirmed with the echo sounder at TB to be at the target position with an accuracy of a few metres (less than 5 metres). The instrument has lithium batteries installed.

The sub-surface solution with a constant velocity profile from the surface to the bottom (U_{max} = 0.5 ms^{-1}) is as follow:

Total Tension on Anchor [kg] = 24.3
Vertical load [kg] = -18.4 Horizontal load [kg] = 15.9
Safe wet anchor mass = 12.1 [kg] = 26.6 [lb]
Safe dry steel anchor mass = 13.9 [kg] = 30.5 [lb]
Safe dry concrete anchor mass = 18.6 [kg] = 40.9 [lb]
Weight under anchor = 4.3 [kg] (negative is down)

The maximum tilt angles for the current profiler under the predefined environmental condition are 4.9, 8.7 for the bottom and top if the instrument, respectively which is in the acceptable tilt range.

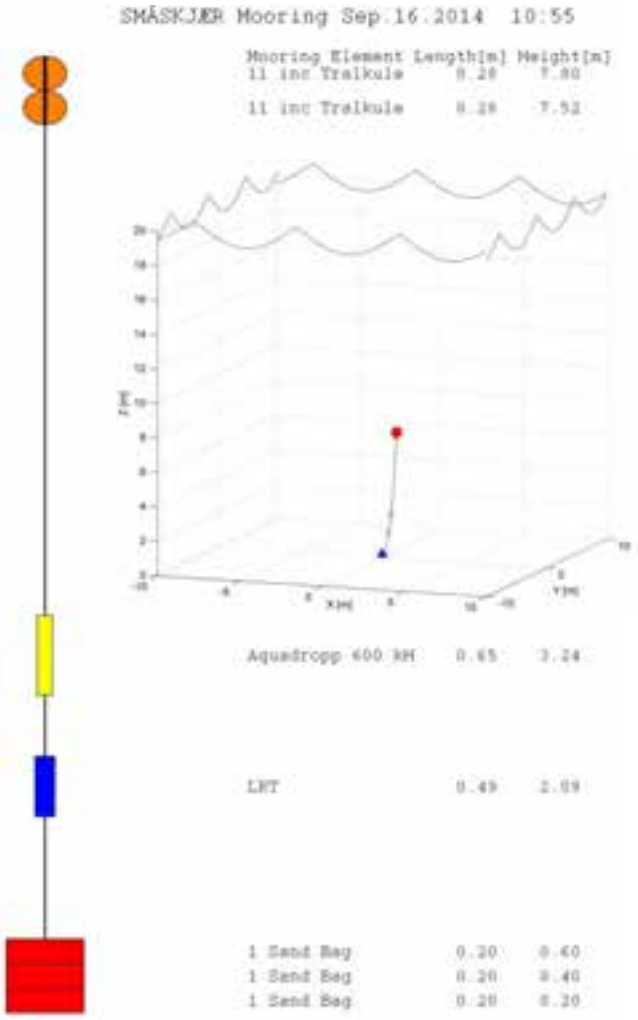

Figure 4. Mooring configuration and the dynamical response at the Småskjær station.

3.2 Station Laksetrappa (Rl1)

Every station needs a name. Laksetrappa is not a local name in the area, but it describes the topography of the location, that takes the shape of a staircase, where the cables are hanging freely above the bottom several places. The water depth at this station is 75 m. A Nortek Aquadopp 400 kHz was deployed approximately 3.2 m over the bottom. The frequency of 400 kHz gives longer vertical range than the instrument with frequency of 600 kHz. A vertical resolution of 3 m was chosen. The instrument gives a reading every 10 minutes, based on measurements during an averaging period. The averaging period was chosen to 220 seconds, giving a precision of 1.7 cm/s. The power setting was set to the highest possible value (HIGH+).

Below the profiling instrument an Aanderaa Seaguard single point current meter was deployed approximately 2.2 m above the bottom. This instrument has higher precision than the profiling instruments, and also has mounted additional instruments measuring conductivity that is used to calculate salinity, pressure, temperature and turbidity.

Above the profiling current meter three 28 cm diameter floats with a positive buoyancy of 8.4 kg each, was attached at the end of a 4 m long rope. Between the current meters a 1 m rope with two 28 cm diameter floats was attached. The rig was weighted down with bio-bags containing approximately 90 kg of gravel. Between the bio-bags and the instrument a transponder with an acoustic release was mounted. The transponder had the identification number LRT3. The deployment of this instrument rig was finished September 16th 12:45 LT (**Figure 5**). Afterwards the position of the rig at the bottom was confirmed with the echo sounder at TB to be at the target position with an accuracy of a few metres (less than 5 metres). The Aquadopp instrument has lithium batteries installed. The Aanderaa Seaguard has alkaline batteries installed.

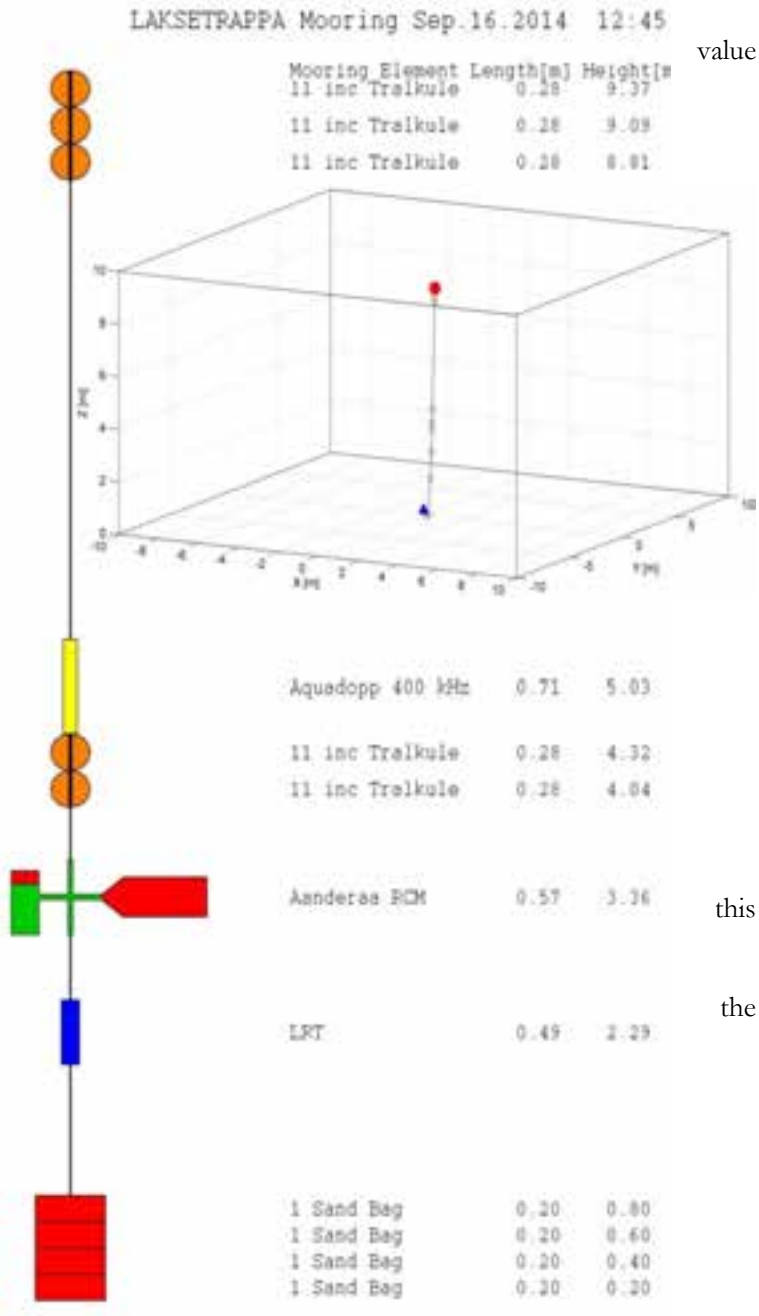

Figure 5. Mooring configuration and the dynamical response at the Laksetrappa station.

The sub-surface solution with a moderate decreasing velocity profile i.e., U_{max} are 0.5, 0.3 and 0.2 ms^{-1} at the surface, mid-depth and the bottom, respectively is as follow:

Total Tension on Anchor [kg] = 41.4
Vertical load [kg] = -40.9 Horizontal load [kg] = 6.8
Safe wet anchor mass = -44.3 [kg] = -97.5 [lb]
Safe dry steel anchor mass = -51.0 [kg] = -112.1 [lb]
Safe dry concrete anchor mass = -68.2 [kg] = -150.1 [lb]
Weight under anchor = 21.4 [kg] (negative is down)

The maximum tilt angles for the current profilers under the predefined environmental condition are 1.6 (bottom)—2.1 (top) for the current profiler (Aquadopp) and 1.5 (bottom)—4.0 (top) for the single point current meter (Aanderaa), respectively which is in the acceptable tilt range.

3.3 Station Botnegrunnen (Rm1)

The water depth at this station is 96 m. A Nortek Continetal 190 kHz was deployed approximately 2.2 m over the bottom. The frequency of 190 kHz gives longer vertical range than the instrument with higher frequency of, but the vertical resolution are coarser. A vertical resolution of 7 m was chosen. The instrument gives a reading every 10 minutes, based on measurements during an averaging period. The averaging period was chosen to 110 seconds, giving a precision of 1.4 cm/s. The power setting was set to the highest possible value (HIGH+).

Above the profiling current meter six 28 cm diameter floats with a positive buoyancy of 8.4 kg each, was attached at the end of a 4 m long rope. The rig was weighted down with bio-bags containing approximately more than 100 kg of gravel. Between the bio-bags and the instrument a transponder with an acoustic release was mounted. The transponder had the identification number LRT4. The deployment of this instrument rig was finished September 16th 14:02 LT (**Figure 6**). Afterwards the position of the rig at the bottom was confirmed with the echo sounder at TB to be at the target position with accuracy of a few metres (less than 5 metres). The instrument has alkaline batteries installed.

The sub-surface solution with a constant velocity profile from the surface to the bottom (U_{max} = 0.5 ms^{-1}) is as follow:

Total Tension on Anchor [kg] = 75.8
Vertical load [kg] = -72.2 Horizontal load [kg] = 23.1
Safe wet anchor mass = -50.4 [kg] = -110.9 [lb]
Safe dry steel anchor mass = -57.9 [kg] = -127.4 [lb]
Safe dry concrete anchor mass = -77.5 [kg] = -170.6 [lb]
Weight under anchor = 55.8 [kg] (negative is down)

The maximum tilt angles for the current profiler under the predefined environmental condition are 3.8 and 13.6 for the bottom and top of the instrument respectively, which is in the acceptable tilt range.

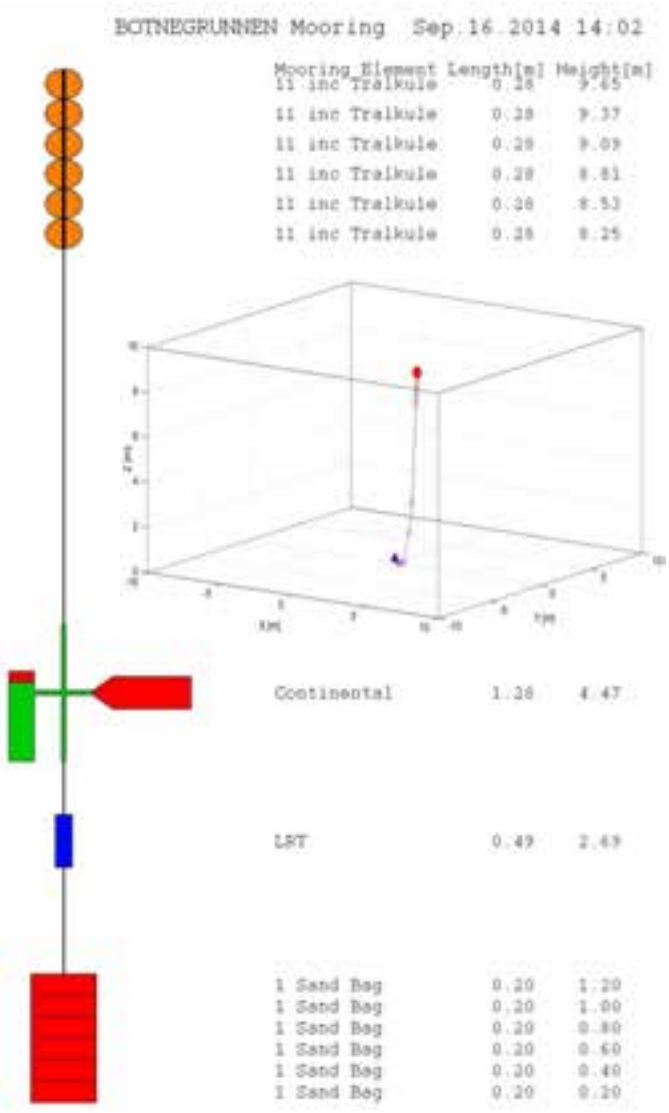

Figure 6. Mooring configuration and the dynamical response at the Botnegrunnen station.

3.4 Station Evje (Rn1)

The water depth at this station is 64 m. A Nortek Aquadopp 400 kHz was deployed approximately 2.2 m over the bottom. A vertical resolution of 3 m was chosen. The instrument gives a reading every 10 minutes, based on measurements during an averaging period. The averaging period was chosen to 240 seconds, giving a precision of 1.6 cm/s. The power setting was set to the highest possible value (HIGH+). Above the current meter two 28 cm diameter floats with a positive buoyancy of 8.4 kg each, was attached at the end of a 4 m long rope. The rig was weighted down with bio-bags containing approximately 90 kg of gravel. Between the bio-bags and the instrument a transponder with an acoustic release was mounted. The transponder had the identification number LRT5. The deployment of this instrument rig was finished September 16th 15:54 LT (**Figure 7**). Afterwards the position of the rig at the bottom was confirmed with the echo sounder at TB to be at the target position with an accuracy of a few metres (less than 5 metres). The instrument has lithium batteries installed.

The sub-surface solution with a constant velocity profile from the surface to the bottom (U_{max} = 0.5 ms^{-1}) is as follow:

Total Tension on Anchor [kg] = 24.3
Vertical load [kg] = -18.4 Horizontal load [kg] = 15.9
Safe wet anchor mass = 12.1 [kg] = 26.6 [lb]
Safe dry steel anchor mass = 13.9 [kg] = 30.5 [lb]
Safe dry concrete anchor mass = 18.6 [kg] = 40.9 [lb]
Weight under anchor = 4.3 [kg] (negative is down)

The maximum tilt angles for the current profiler under the predefined environmental condition are 4.5 and 8.7 for the bottom and top of the instrument respectively, which is in the acceptable tilt range.

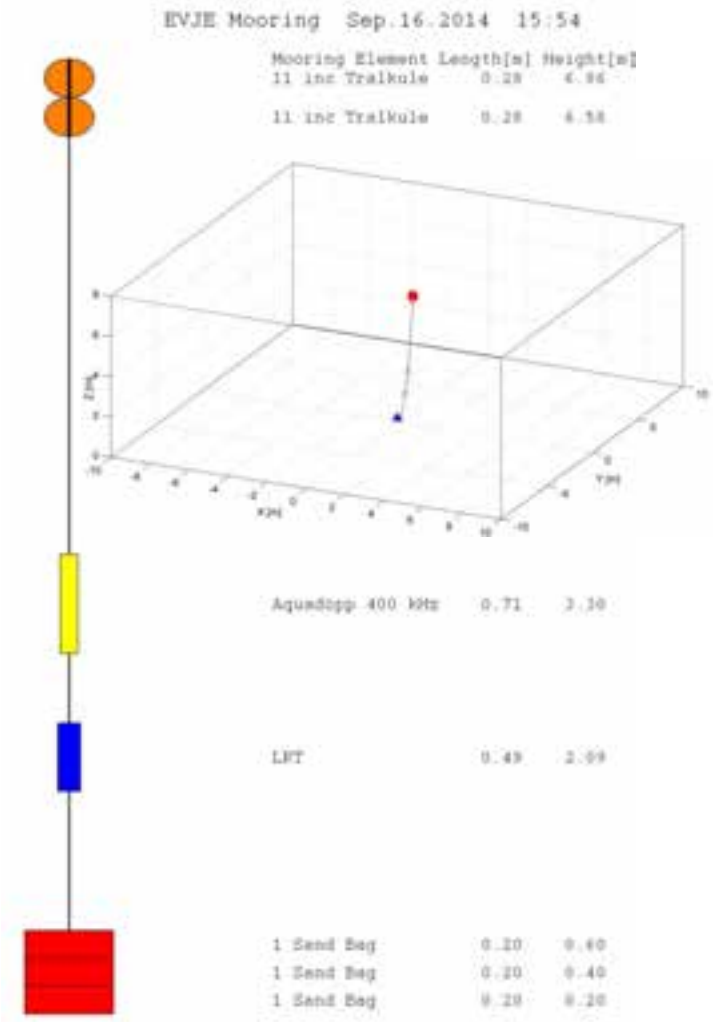

Figure 7. Mooring configuration and the dynamical response at the Evje station.

3.5 Station Filtvedt (Km1)

The water depth at this station is 153 m. A Nortek Continental 190 kHz was deployed approximately 2.2 m over the bottom. A vertical resolution of 5 m was chosen. The instrument gives a reading every 10 minutes, based on measurements during an averaging period. The averaging period was chosen to 220 seconds, giving a precision of 1.4 cm/s. The power setting was set to the highest possible value (HIGH+). Above the current meter six 28 cm diameter floats with a positive buoyancy of 8.4 kg each, was attached at the end of a 4 m long rope. The rig was weighted down with bio-bags containing approximately 100 kg of gravel. Between the bio-bags and the instrument a transponder with an acoustic release was mounted. The transponder had the identification number 203-2. The deployment of this instrument rig was finished September 17th approximately 15:51 LT (**Figure 8**). Afterwards the position of the rig at the bottom was confirmed with the echo sounder at TB to be at the target position with an accuracy of a few metres (less than 5 metres). The instrument has lithium batteries installed.

The sub-surface solution with a constant velocity profile from the surface to the bottom (U_{max} = 0.5 ms^{-1}) is as follow:

Total Tension on Anchor [kg] = 78.8
Vertical load [kg] = -75.2 Horizontal load [kg] = 23.5
Safe wet anchor mass = -53.9 [kg] = -118.6 [lb]
Safe dry steel anchor mass = -62.0 [kg] = -136.3 [lb]
Safe dry concrete anchor mass = -82.9 [kg] = -182.5 [lb]
Weight under anchor = 58.8 [kg] (negative is down).

The maximum tilt angles for the current profiler under the predefined environmental condition are 3.7 and 15.3 for the bottom and top of the instrument respectively, which is in the acceptable tilt range.

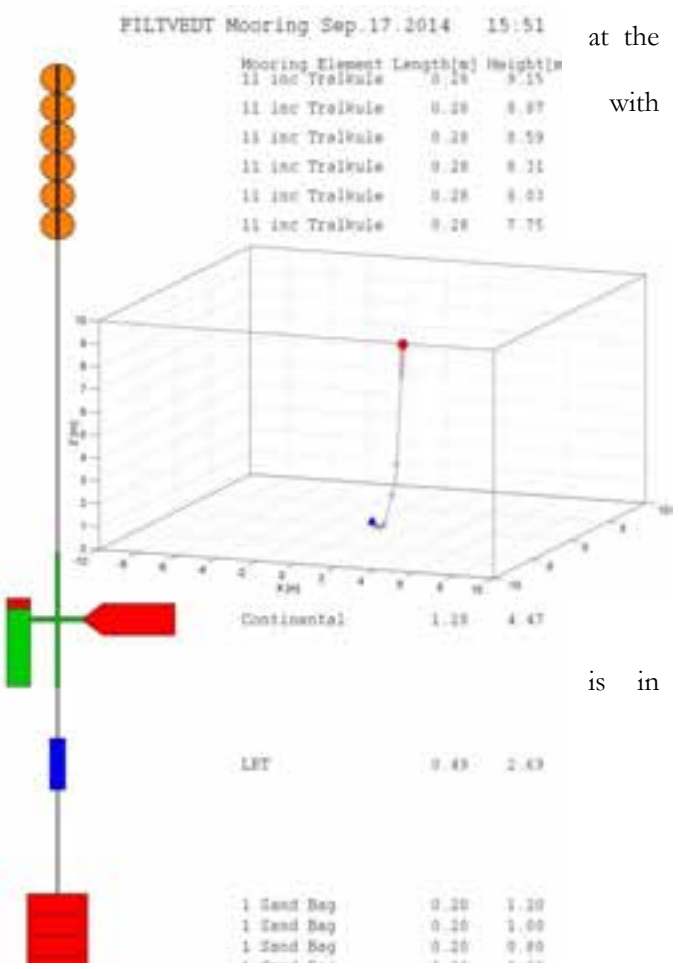

Figure 8. Mooring configuration and the dynamical response at the Filtvedt station.

3.6 Station Brenntangen (Kn2)

The water depth at this station is 54 m. The mooring at this station is identical to the mooring at Evje. Therefore, the same design and configuration is applied to the both stations. A Nortek Aquadopp 400 kHz was deployed approximately 2.2 m over the bottom. A vertical resolution of 3 m was chosen. The instrument gives a reading every 10 minutes, based on measurements during an averaging period. The averaging period was chosen to 240 seconds, giving a precision of 1.6 cm/s. The power setting was set to the highest possible value (HIGH+).

Above the current meter two 28 cm diameter floats with a positive buoyancy of 8.4 kg each, was attached at the end of a 4 m long rope. The rig was weighted down with bio-bags containing approximately 90 kg of gravel. Between the bio-bags and the instrument a transponder with an acoustic release was mounted. The transponder had the identification number LRT5. The deployment of this instrument rig was finished September 16th 15:00 LT (**Figure 9**). Afterwards the position of the rig at the bottom was confirmed with the echo sounder at TB to be at the target position with an accuracy of a few metres (less than 5 metres). The instrument has lithium batteries installed.

The sub-surface solution with a constant velocity profile from the surface to the bottom (U_{max} = 0.5 ms^{-1}) is as follow:

Total Tension on Anchor [kg] = 24.3
Vertical load [kg] = -18.4 Horizontal load [kg] = 15.9
Safe wet anchor mass = 12.1 [kg] = 26.6 [lb]
Safe dry steel anchor mass = 13.9 [kg] = 30.5 [lb]
Safe dry concrete anchor mass = 18.6 [kg] = 40.9 [lb]
Weight under anchor = 4.3 [kg] (negative is down)

The maximum tilt angles for the current profiler under the predefined environmental condition are 4.5 and 8.7 for the bottom and top of the instrument respectively, which is in the acceptable tilt range.

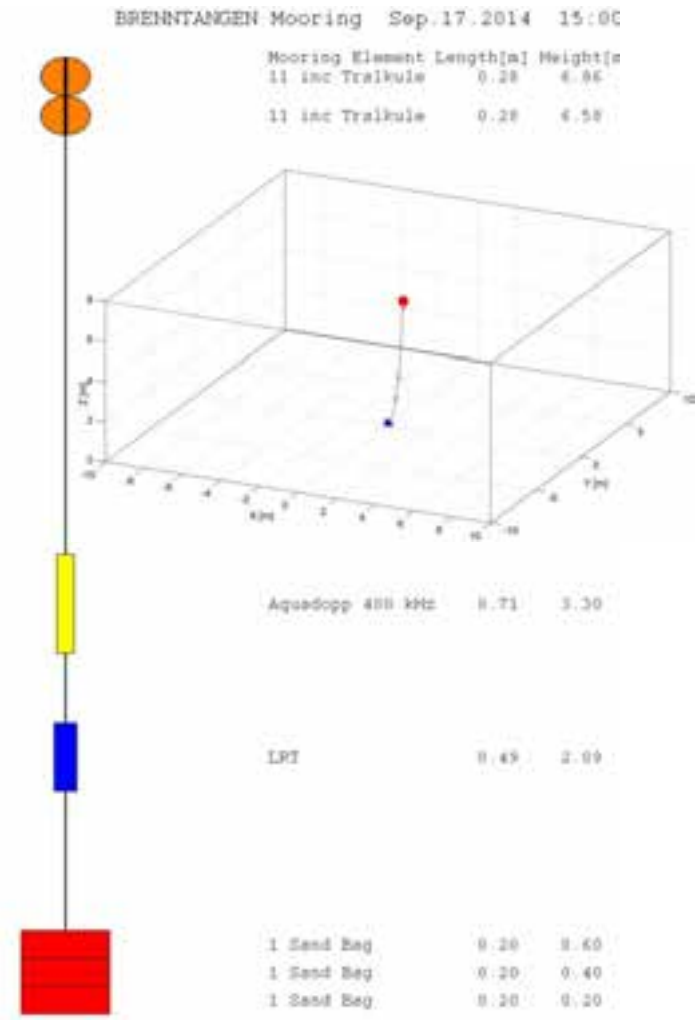

Figure 9. Mooring configuration and the dynamical response at the Brenntangen station.

4. Results

4.1 Variation in the driving forces

The forces that cause the observed current conditions were discussed in chapter 2.2. The list below summarizes the driving forces:

1. Atmospheric pressure
2. Wind
3. Sea level
4. River discharge
5. Influence from the open ocean

As mentioned earlier an atmospheric low pressure will cause a sea level rise (storm surge), and in **Figure 10** the sea level and the amplitude of the sea level oscillation is plotted as a time series together with the atmospheric pressure at Rygge Airport and also the wind speed at Gullholmen. The amplitude of the sea level oscillations can be calculated by finding the difference of the maximum and the minimum sea level during a tidal cycle, and divide by two. As can be seen from **Figure 10**, there was two storm surge events September 27th and October 22nd. The first storm surge event did not cause an increase in sea level amplitude, but during the second event the amplitude was 0.45 m.

The barotropic forcing is associated with changes in sea level, and the amplitude of sea level is a measure of the strength of the barotropic forcing. **Figure 11** shows a cumulative plot of the sea level amplitude at the station Oscarsborg (N 59°40.683' E 10°36.283'). The cumulative plot gives percentage of the measurements below a given value. For example in 95 % of the observations the amplitude is lower than 27.2 cm (95 percentile). The 99 percentile is 33.3 cm. This means that the amplitude is more than 33.3 cm during 14-22 of all the tidal cycles during a year, assuming that the duration of the in- or outflow is between 4 and 6 hours.

The maximum amplitude is almost 70 cm is in connection with storm surge events, and might happen a few times each year. The duration of episodes with such strong barotropic forcing is typically less than 6 hours. In **Figure 12** the frequency distribution for the same data set is plotted as a histogram. Only 0.006 % of the observations have the highest amplitude (66.3-67.5 cm). Assuming that the duration of a storm surge event is a little less than 6 hours, this happens only one or two times during a period of 14 years.

River discharge especially from Drammenselva, is important for currents near the surface. Unfortunately river discharge from Drammmenselva was not available at the time of writing of this report, but river flow is measured at the station Mjøndalen Bru.

Observations of temperature and salinity profiles are not available with a sufficient time resolution, and because of this it is not possible to associate observed currents to for example inflow of water from Skagerrak. CTD profiles from three instances in time are shown in **Figure 13**. From the figure it can be seen that the horizontal difference between the stations OF-4 and OF-7b is small below approximately 100 m depth.

In the rest of this chapter the observed currents at each of the six stations in Table 1 will be shown, with focus on the currents near the bottom.

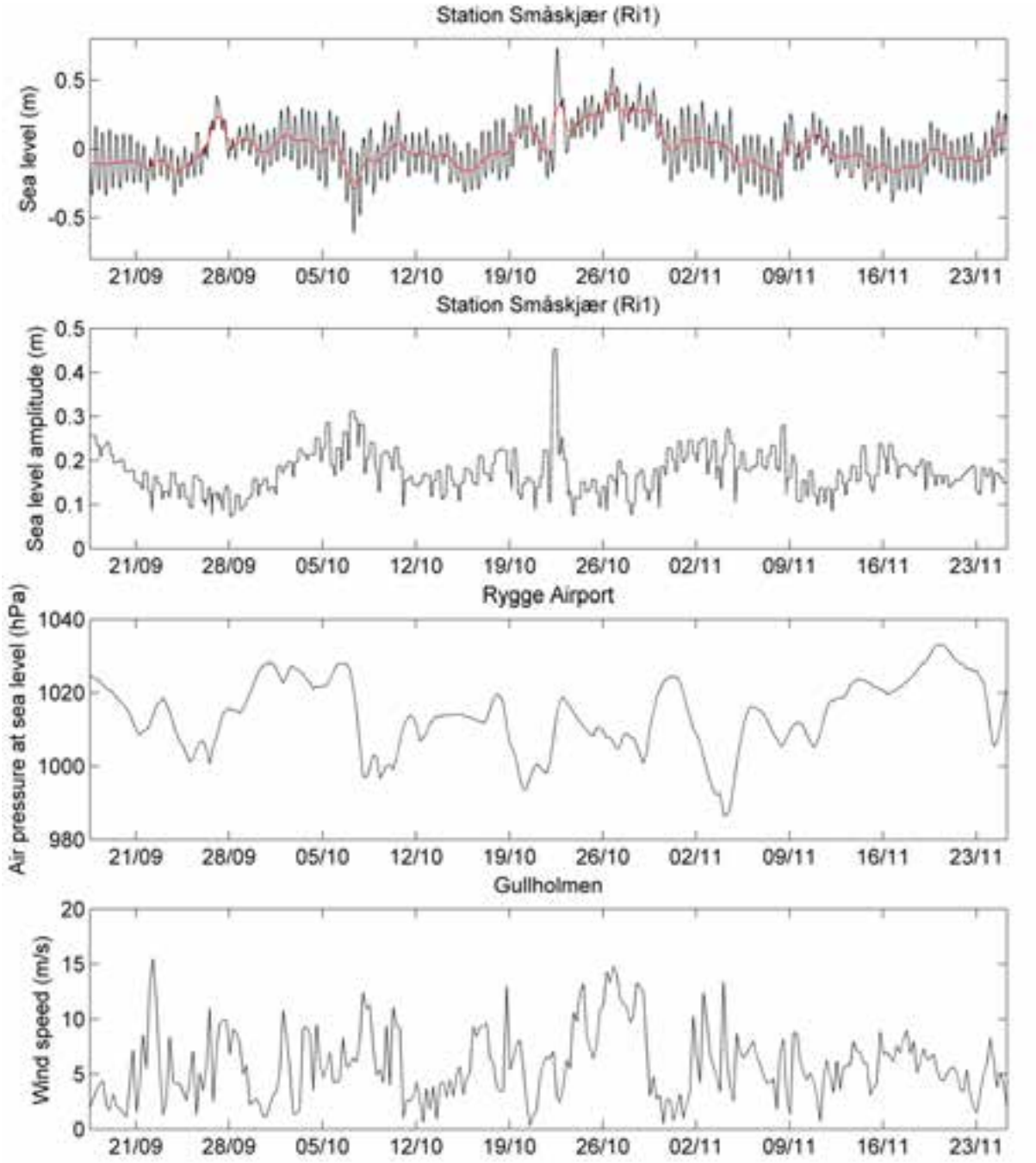

Figure 10. Sea level at station Ri1 from September to November 2014 is shown in the upper panel, with the calculated sea level amplitude below. The red line is a 25 hour running mean. Atmospheric pressure at Rygge Airport is shown in the third panel and wind speed at the station Gullholmen is shown in the lower panel.

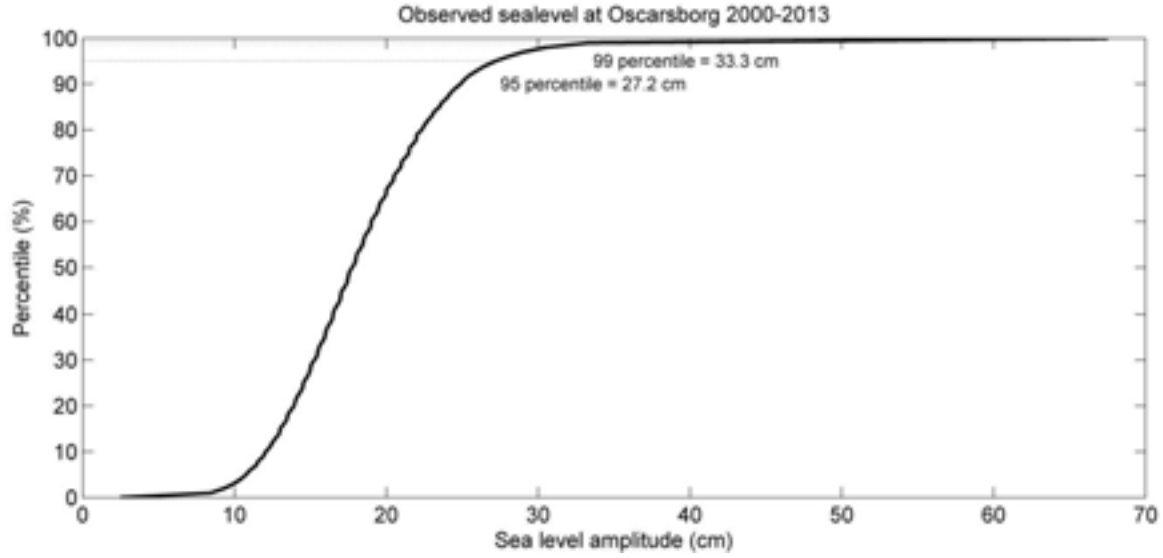

Figure 11. Cumulative plot of sea level amplitude for the period 2000-2013 at the station Oscarsborg.

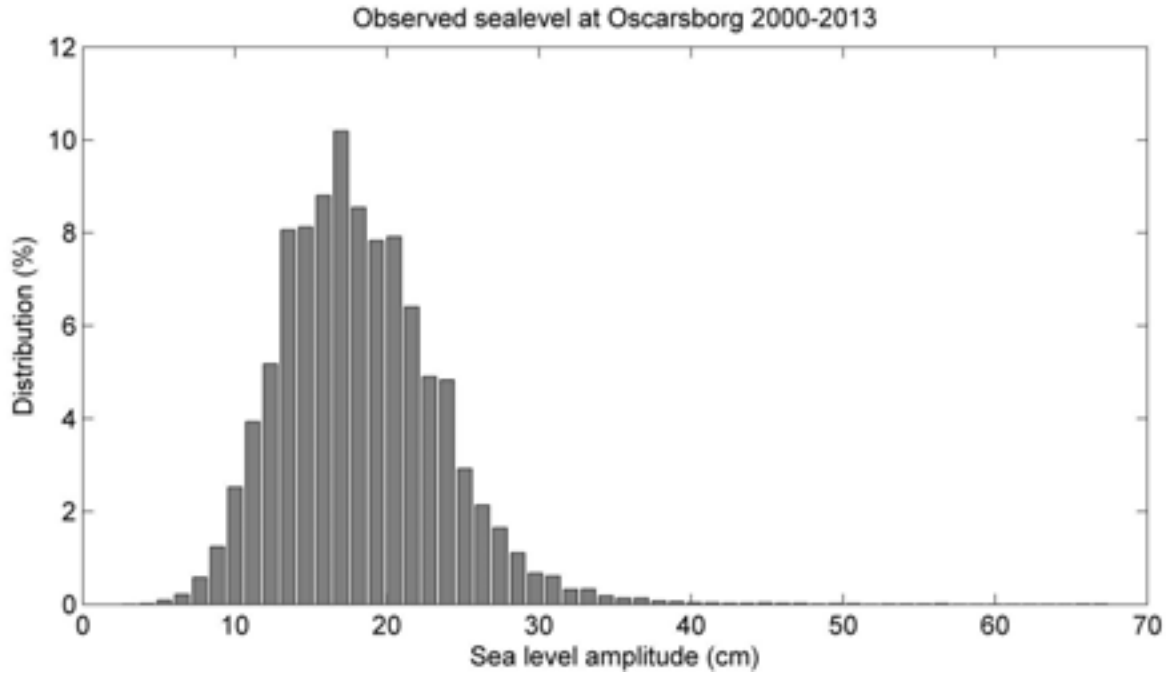

Figure 12. Frequency distribution for the sea level amplitude for the period 2000-2013 at the station Oscarsborg.

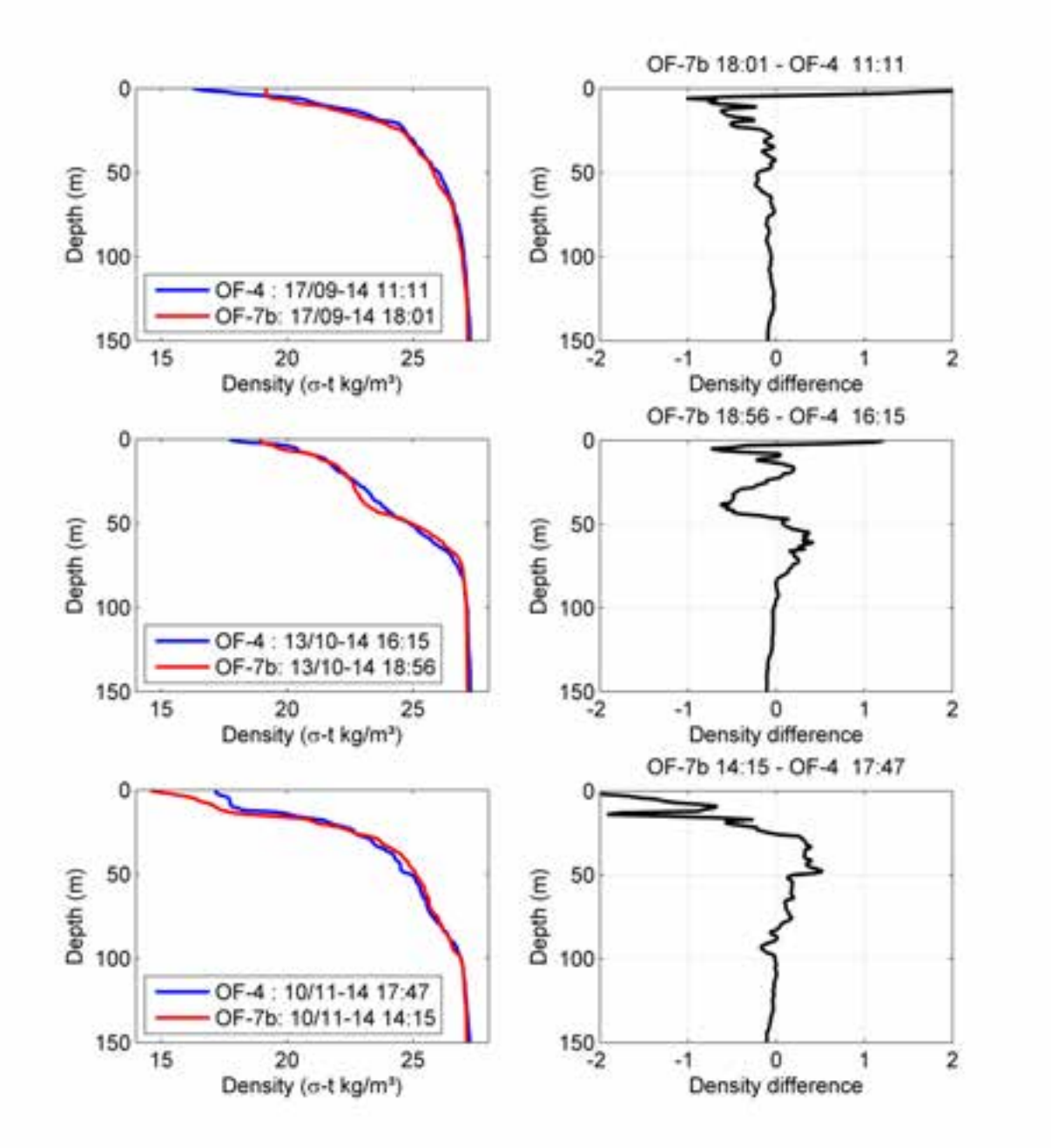

Figure 13. Density profiles from the stations OF-4 and OF-7b at three instances in time (left column). Horizontal density difference between the two stations (right column).

4.2 Station Småskjær (Ri1)

At Småskjær the highest observed current speeds (0.88 m/s) are found near the surface (4.5 m depth) and the direction of the strongest currents is south-easterly (**Figure 14** and **Table 4**). This is probably caused by river discharge from the river Drammenselva (estuarine circulation), but is not verified by correlating the surface current with river discharge. Most of the observed variability near the surface can be explained by a mean flow and a tidal signal.

The highest observed current speed near the bottom was 0.24 m/s (**Figure 15** and **Table 4**). The water depth at this station is 20 m, so this was 3.5 m over the bottom. The highest currents was in the north-south direction, and seems to happen in connection with high sea level amplitudes. However, relatively high current speeds near the bottom occurred two tidal cycles after the storm surge event October 22nd (**Figure 16**). Most of the current variability near the bottom has irregular periods of less than 25 hours.

Table 4. Maximum current at each depth at station Småskjær.

Depth (m)	Observed current (m/s)	Tidal current (m/s)	Lowpass 25 hrs current (m/s)
4.5	0.88	0.13	0.50
6.5	0.86	0.10	0.53
8.5	0.73	0.08	0.51
10.5	0.65	0.05	0.38
12.5	0.40	0.03	0.19
14.5	0.23	0.03	0.09
16.5	0.24	0.02	0.06

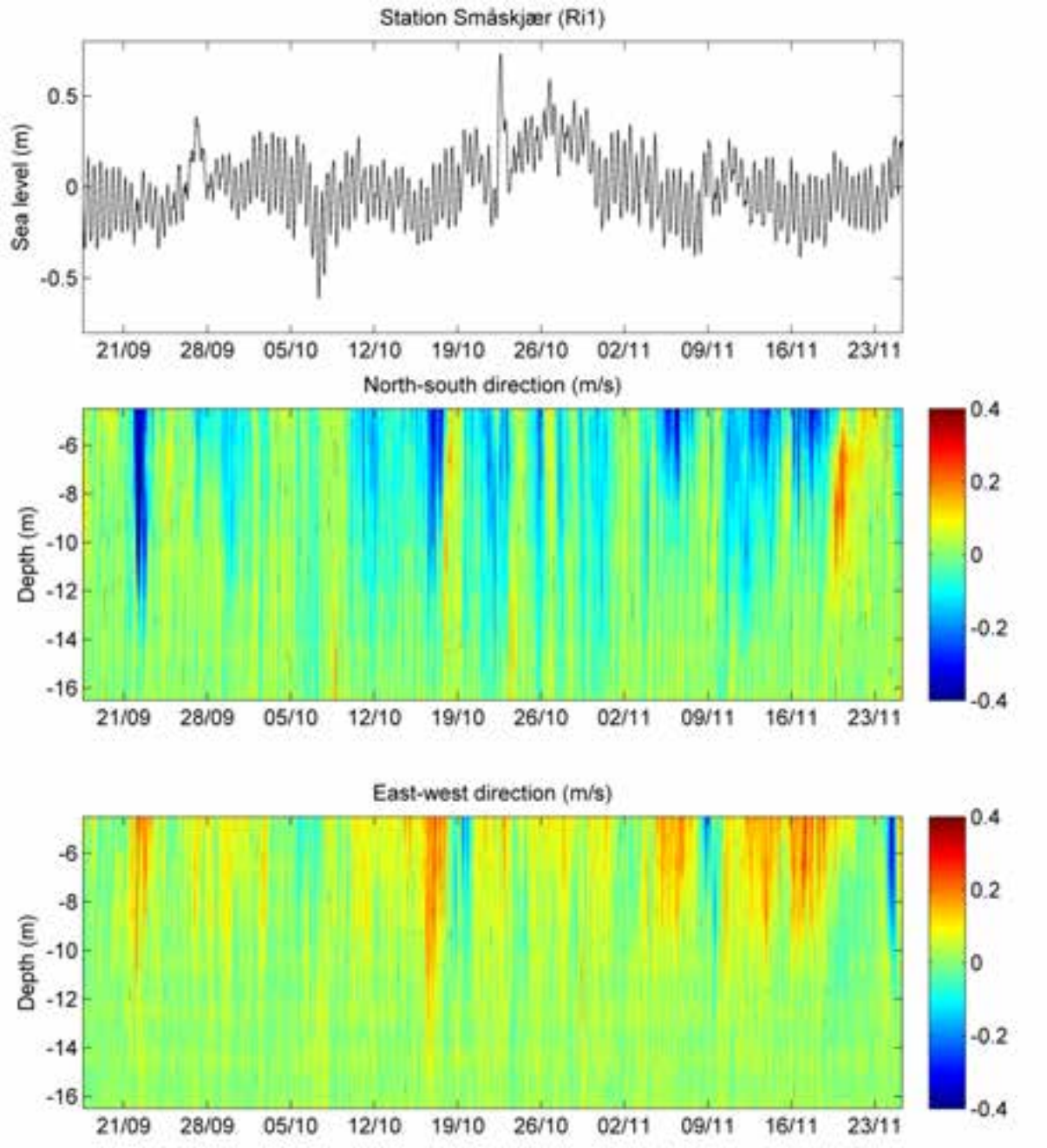

Figure 14. Sea level (upper panel), current in the north-south direction (middle panel) and current in the east-west direction at the station Småskjær (Ri1) from September to November 2014.

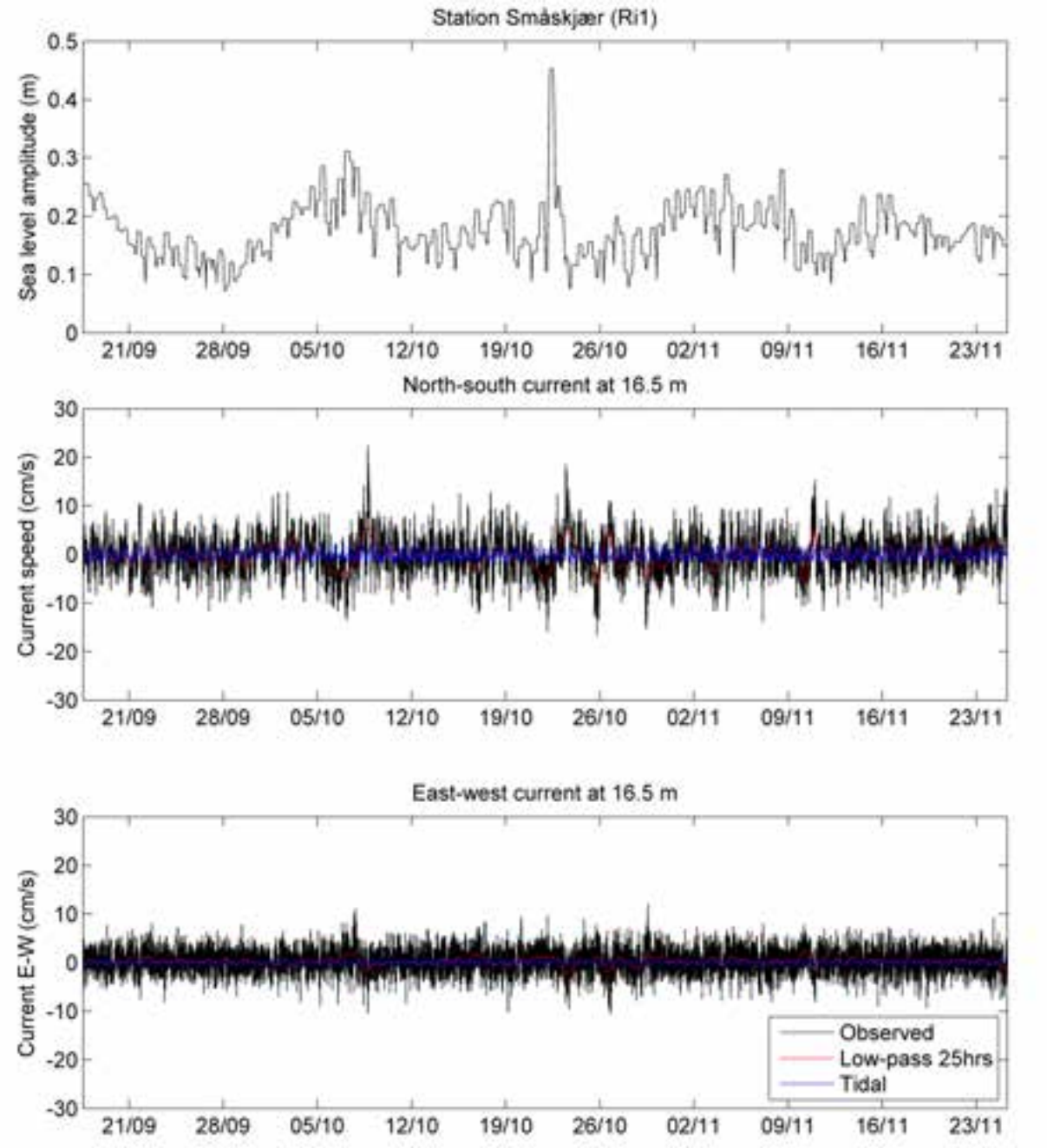

Figure 15. The current 3.5 m over the bottom at station Småskjær from September to November 2014 (middle and lower panel) plotted as a time series together with the sea level amplitude.

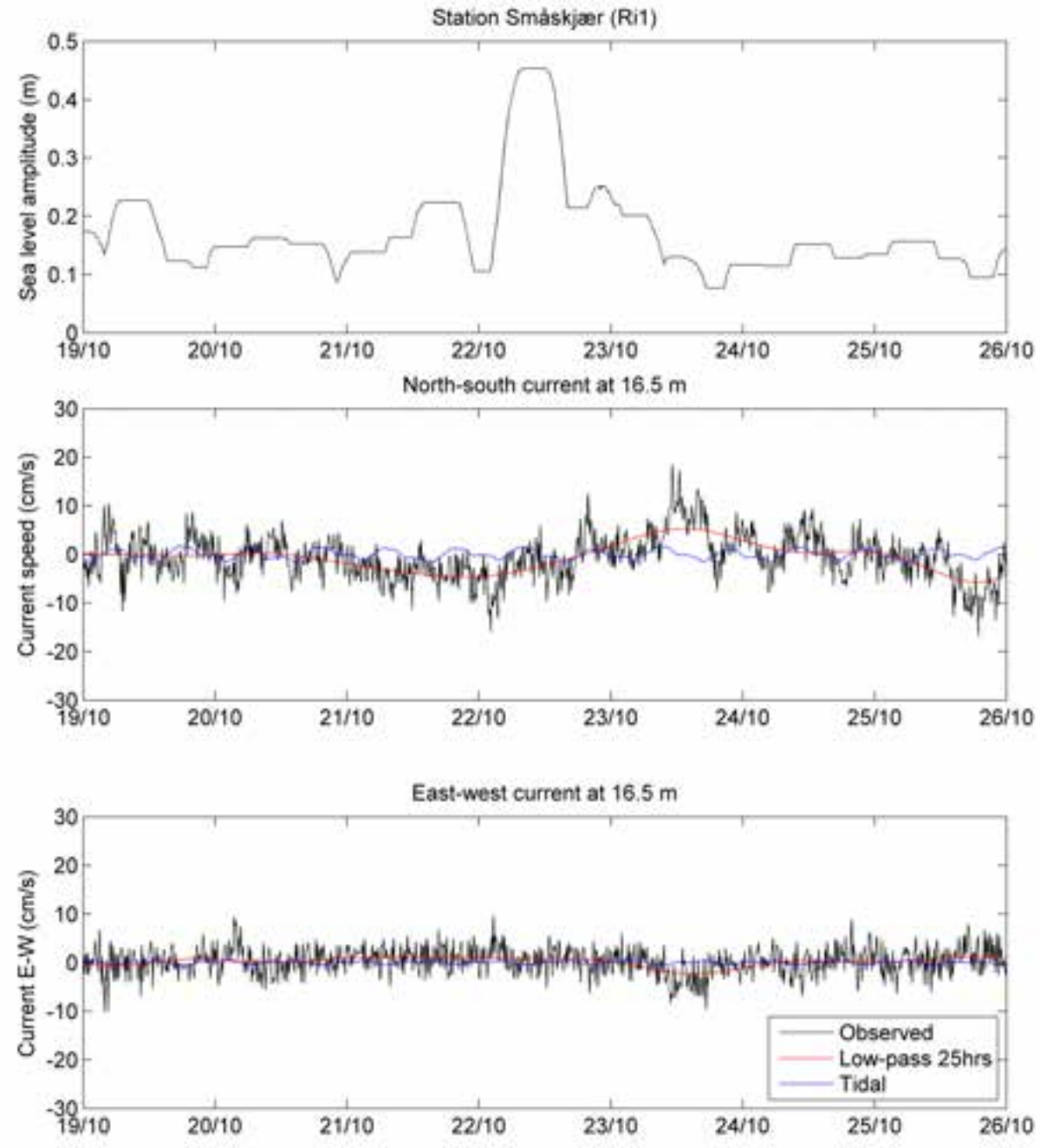

Figure 16. The current 3.5 m over the bottom at station Småskjær (middle and lower panel) plotted as a time series together with the sea level amplitude.

4.3 Station Laksetrappa (Rl1)

At Laksetrappa the highest observed current speeds (0.73 m/s) are found in the upper layer (10 m depth) and is in the north-south direction (**Figure 17** and **Table 5**). Most of the observed variability near the surface can be explained by a mean flow and a tidal signal.

The highest observed current speed at the deepest cell of the ADCP measurements was 0.21 m/s (**Figure 18** and **Table 5**). The water depth at this station is approximately 76 m, so this was 9 m over the bottom. A single point measurement was deployed 3 m over the bottom, and the maximum current speed was a little lower (0.20 m/s, **Figure 19** and **Table 5**). The sea level amplitude was relatively low when the highest currents occurred (**Figure 20**). Most of the current variability near the bottom has irregular periods of less than 25 hours.

Table 5. Maximum current at each depth at station Laksetrappa.

Depth (m)	Observed current (m/s)	Tidal current (m/s)	Lowpass 25 hrs current (m/s)
10	0.73	0.16	0.50
13	0.58	0.13	0.43
16	0.46	0.03	0.31
19	0.34	0.04	0.25
22	0.39	0.04	0.31
25	0.48	0.05	0.38
28	0.47	0.04	0.34
31	0.43	0.04	0.31
34	0.34	0.08	0.24
37	0.31	0.07	0.22
40	0.32	0.07	0.19
43	0.30	0.07	0.18
46	0.28	0.08	0.20
49	0.31	0.07	0.21
52	0.27	0.08	0.17
55	0.22	0.04	0.14
58	0.23	0.04	0.14
61	0.25	0.06	0.12
64	0.19	0.05	0.10
67	0.21	0.03	0.09
73	0.20	0.02	0.05

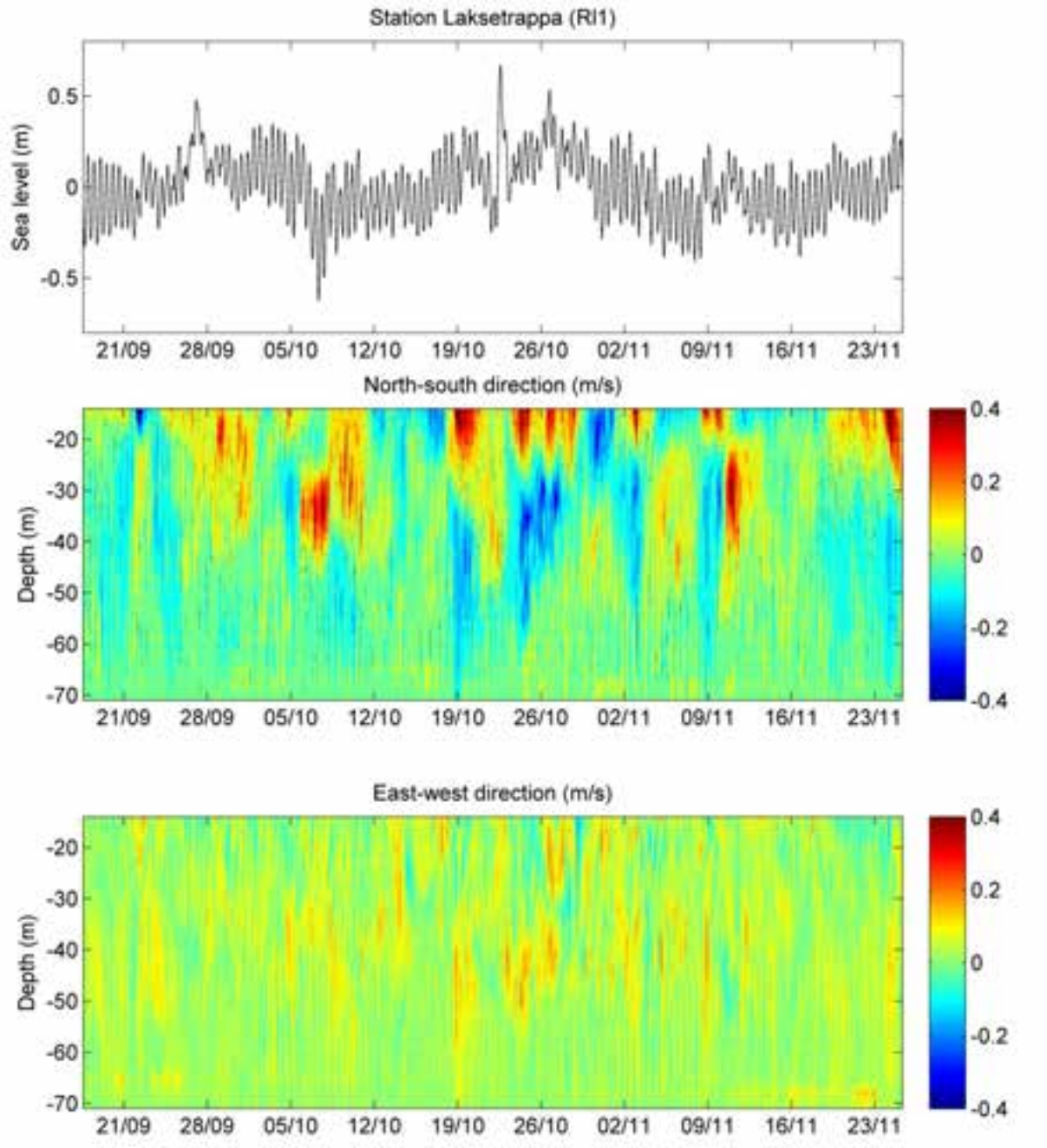

Figure 17. Sea level (upper panel), current in the north-south direction (middle panel) and current in the east-west direction at the station Laksetrappa (Rl1) from September to November 2014.

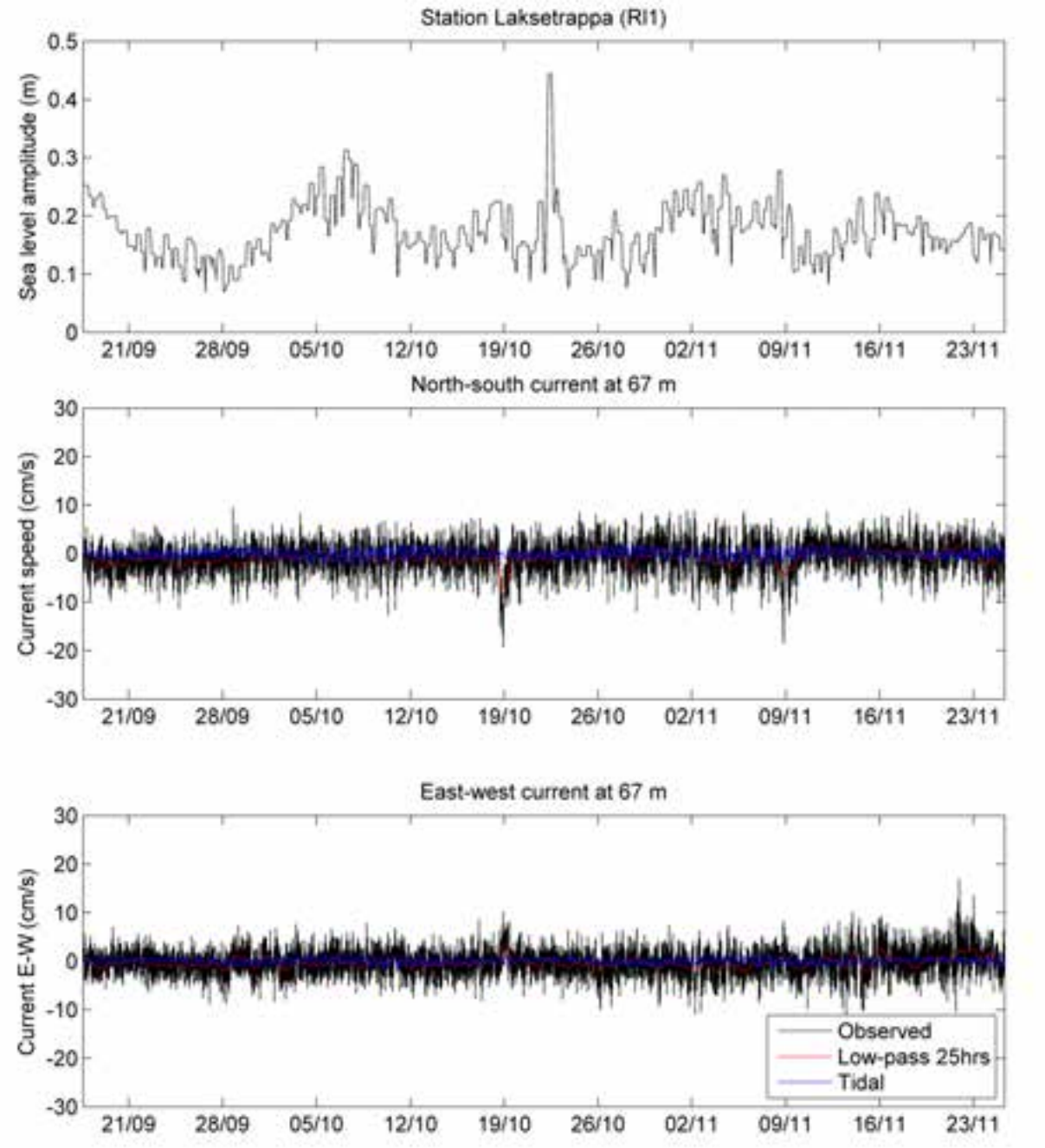

Figure 18. The current 9 m over the bottom at station Laksetrappa from September to November 2014 (middle and lower panel) plotted as a time series together with the sea level amplitude.

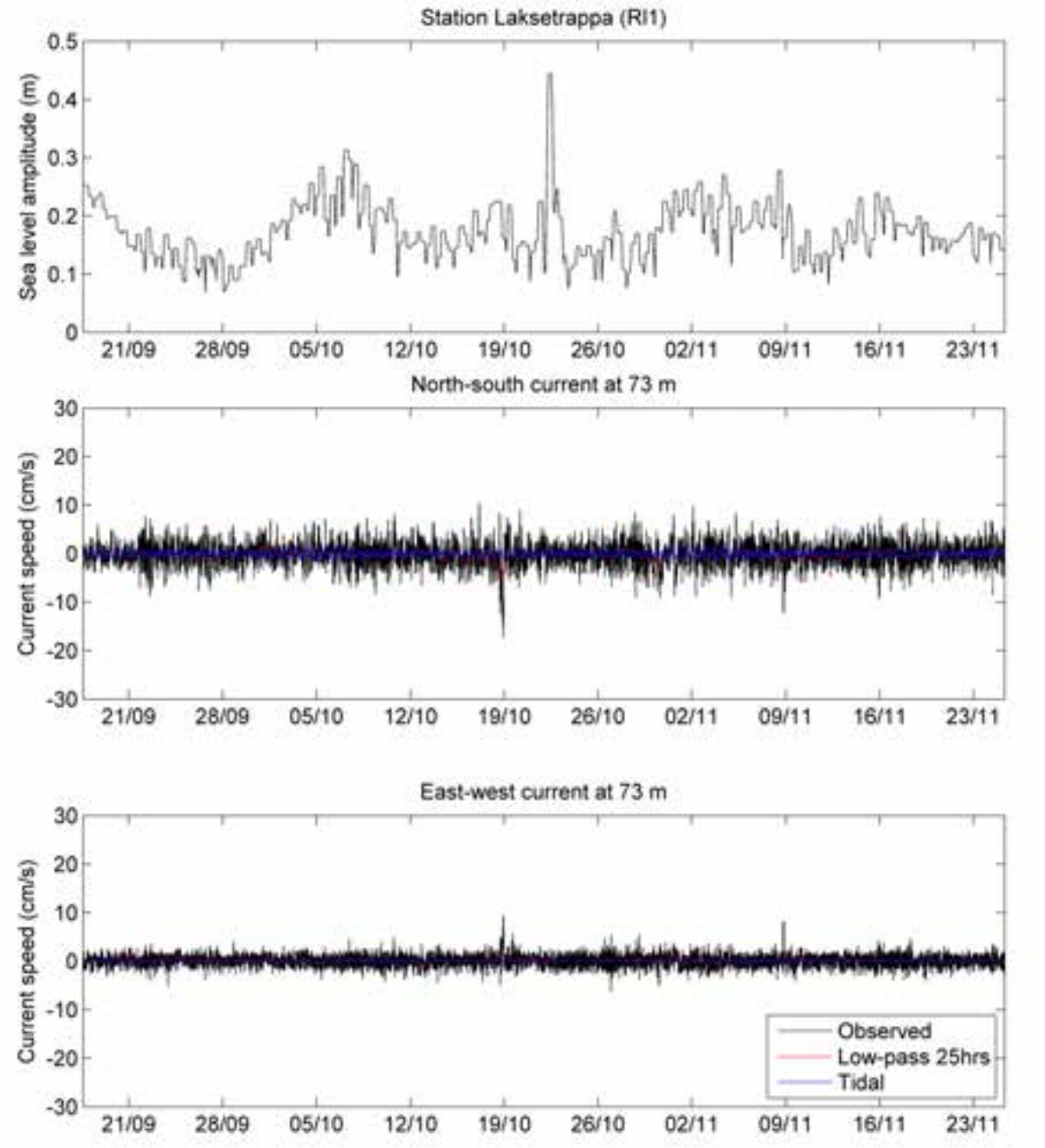

Figure 19. The current 3 m over the bottom at station Laksetrappa (middle and lower panel) plotted as a time series together with the sea level amplitude.

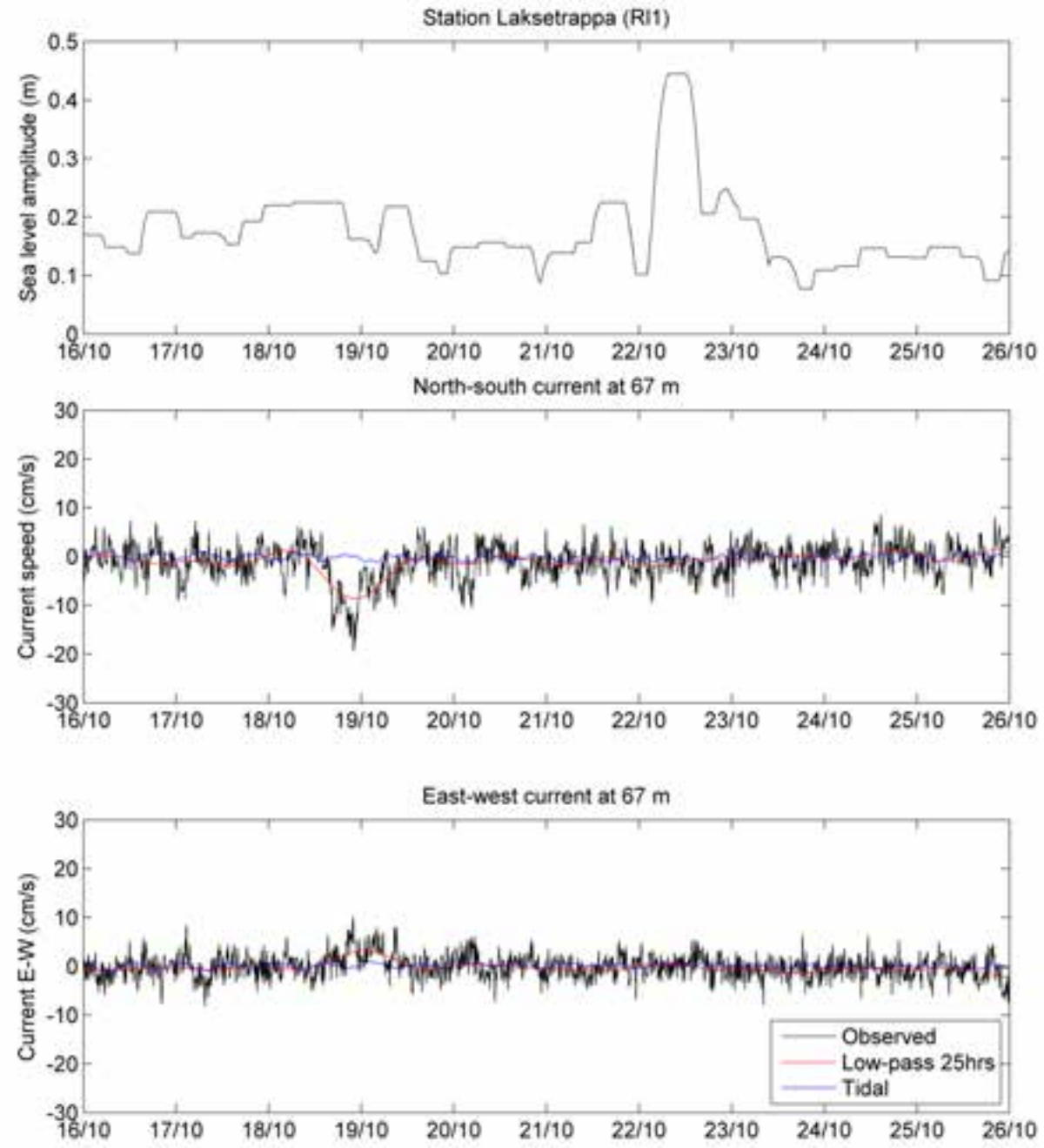

Figure 20. The current 9 m over the bottom at station Laksetrappa (middle and lower panel) plotted as a time series together with the sea level amplitude.

4.4 Station Botnegrunnen (Rm1)

At Botnegrunnen the highest observed current speeds (0.42 m/s) are found at 69 m depth in the east-west direction (**Figure 21** and **Table 6**). It is probable that the bathymetry plays an important role for the observed currents at this station. Most of the current variability at this depth has irregular periods of less than 25 hours. Currents further up in the water column are more influenced by periods with longer duration.

The highest observed current speed at the deepest cell of the ADCP measurements was 0.15 m/s (**Figure 22** and **Table 6**). The water depth at this station is approximately 96 m, so this was 13 m over the bottom. The direction of the current at this depth was easterly (**Figure 23**). Most of the current variability near the bottom has irregular periods of less than 25 hours.

Table 6. Maximum current at each depth at station Botnegrunnen.

Depth (m)	Observed current (m/s)	Tidal current (m/s)	Lowpass 25 hrs current (m/s)
13	0.34	0.04	0.19
20	0.31	0.05	0.22
27	0.33	0.08	0.19
34	0.31	0.11	0.20
41	0.36	0.10	0.17
48	0.25	0.06	0.11
55	0.22	0.03	0.07
62	0.32	0.04	0.06
69	0.42	0.04	0.10
76	0.37	0.03	0.08
83	0.15	0.01	0.05

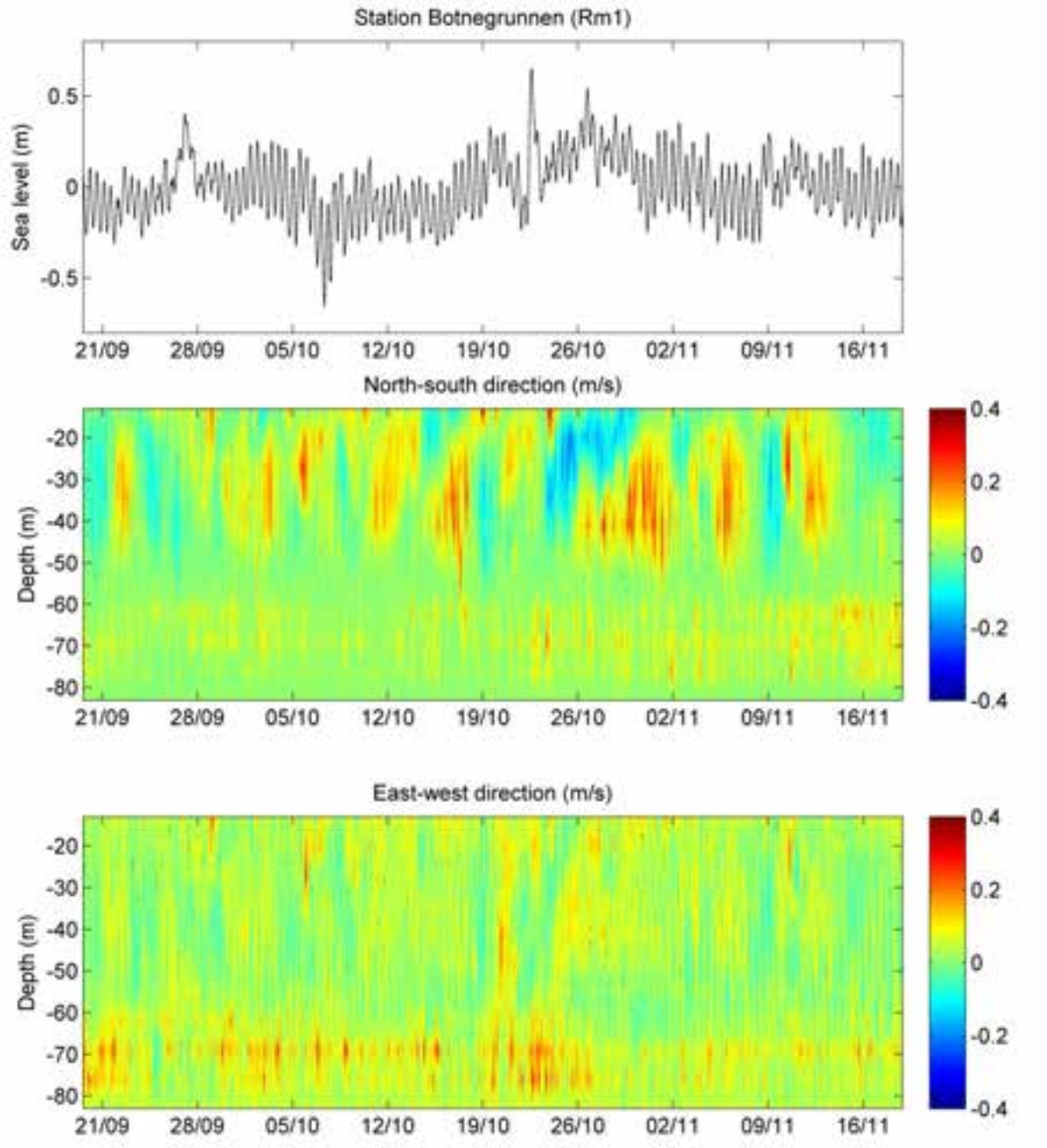

Figure 21. Sea level (upper panel), current in the north-south direction (middle panel) and current in the east-west direction at the station Botnegrunnen (Rm1) from September to November 2014.

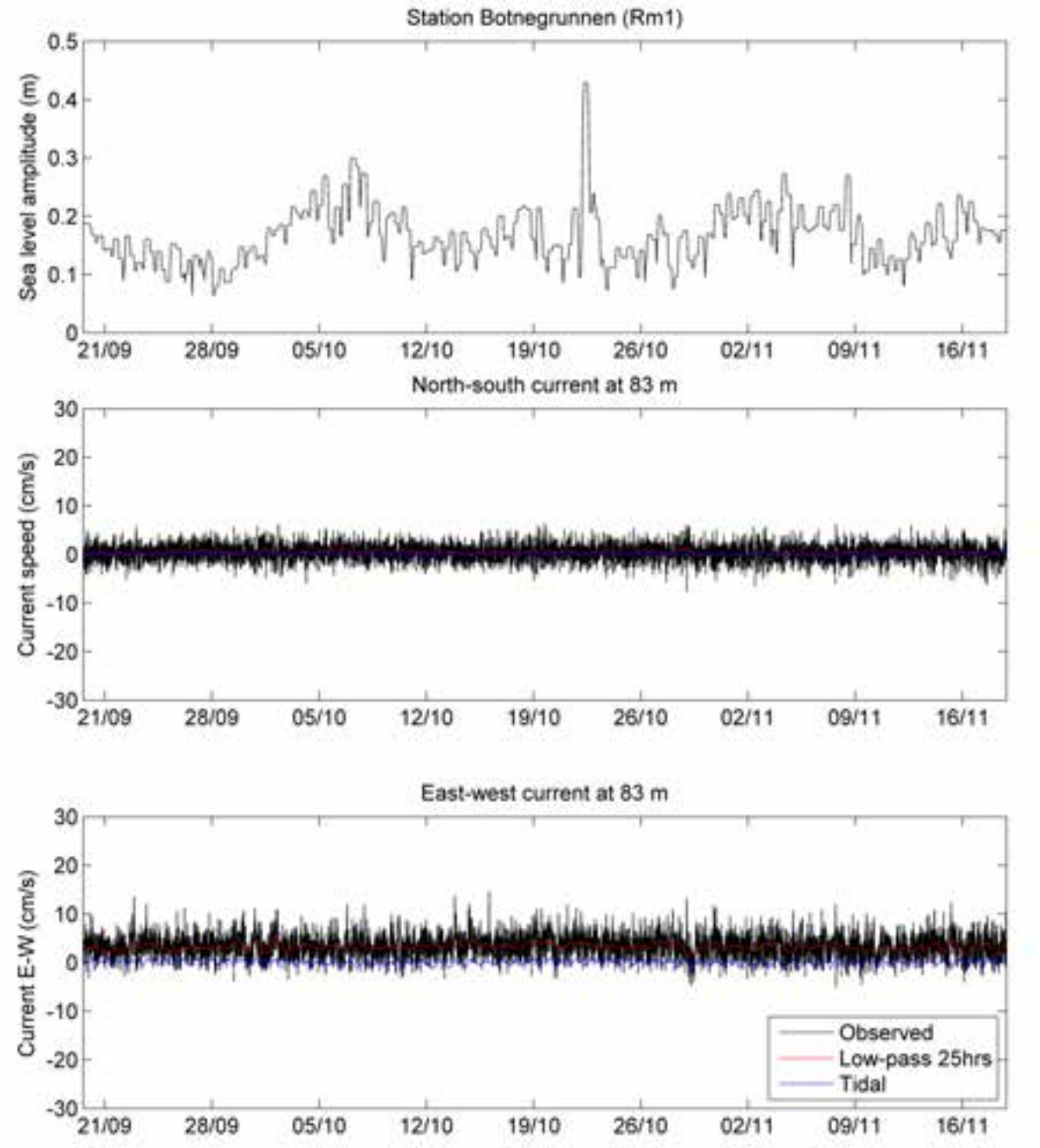

Figure 22. The current 13 m over the bottom at station Botnegrunnen (middle and lower panel) from September to November 2014 plotted as a time series together with the sea level amplitude.

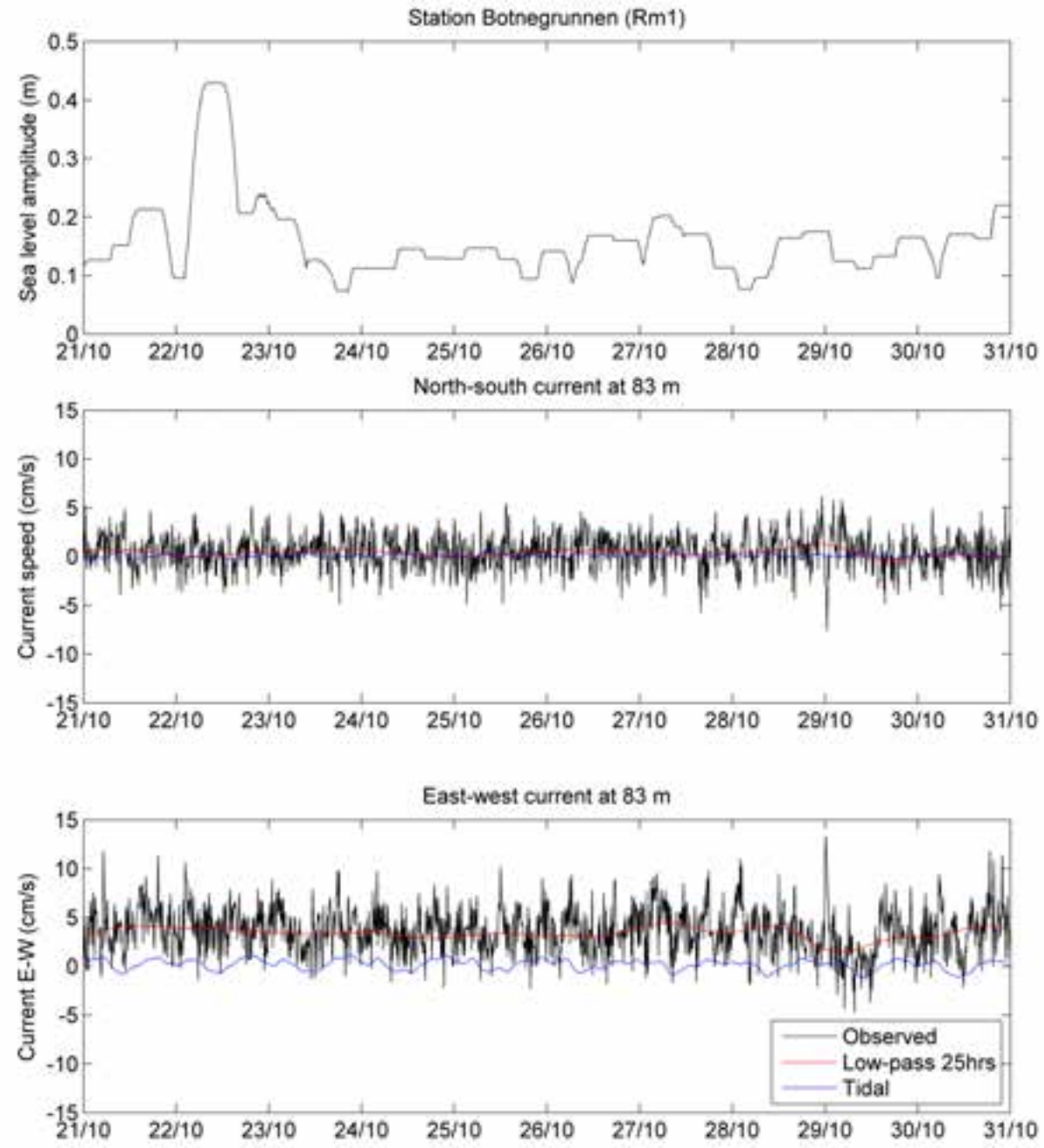

Figure 23. The current 13 m over the bottom at station Botnegrunnen (middle and lower panel) plotted as a time series together with the sea level amplitude.

4.5 Station Evje (Rn1)

At Evje the highest observed current speeds (0.40 m/s) are found at 37 m depth in the north-south direction (**Figure 24** and **Table 7**). Most of the current variability at this depth has irregular periods of less than 25 hours.

The highest observed current speed at the deepest cell of the ADCP measurements was 0.16 m/s (**Figure 25** and **Table 7**). The water depth at this station is approximately 64 m, so this was 6 m over the bottom. Most of the current variability near the bottom has irregular periods of less than 25 hours. The highest currents near the bottom were observed in the north-south direction (**Figure 26**).

Table 7. Maximum current at each depth at station Evje.

Depth (m)	Observed current (m/s)	Tidal current (m/s)	Lowpass 25 hrs current (m/s)
7	0.33	0.05	0.14
10	0.29	0.04	0.11
13	0.32	0.03	0.11
16	0.31	0.03	0.12
19	0.24	0.03	0.13
22	0.27	0.03	0.12
25	0.22	0.03	0.08
28	0.19	0.02	0.05
31	0.26	0.03	0.04
34	0.35	0.02	0.09
37	0.40	0.02	0.12
40	0.34	0.04	0.11
43	0.30	0.03	0.08
46	0.22	0.02	0.05
49	0.20	0.01	0.03
52	0.20	0.01	0.03
55	0.21	0.01	0.03
58	0.16	0.01	0.03

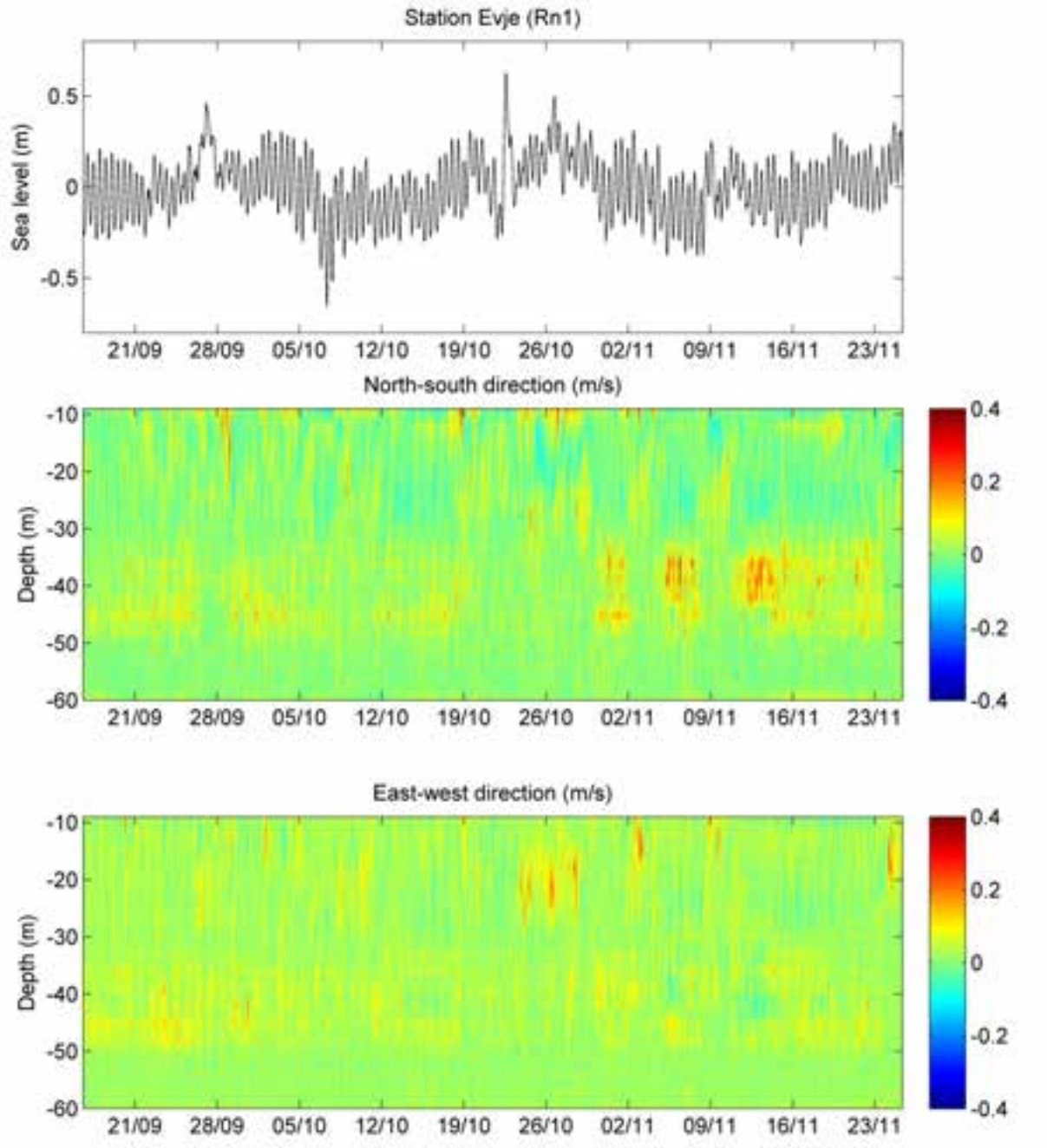

Figure 24. Sea level (upper panel), current in the north-south direction (middle panel) and current in the east-west direction at the station Evje (Rn1) from September to November 2014.

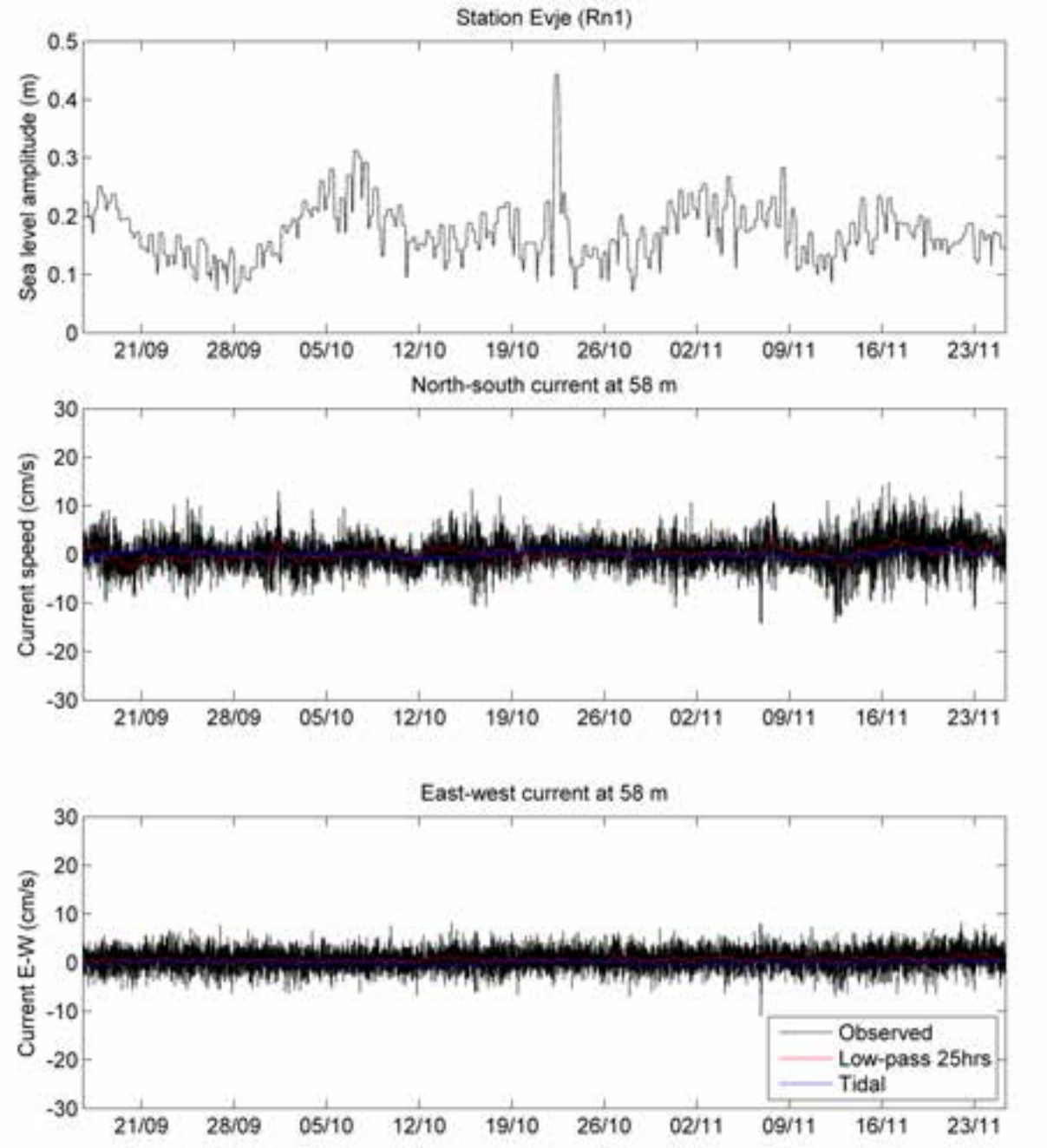

Figure 25. The current 6 m over the bottom at station Evje (middle and lower panel) from September to November 2014 plotted as a time series together with the sea level amplitude.

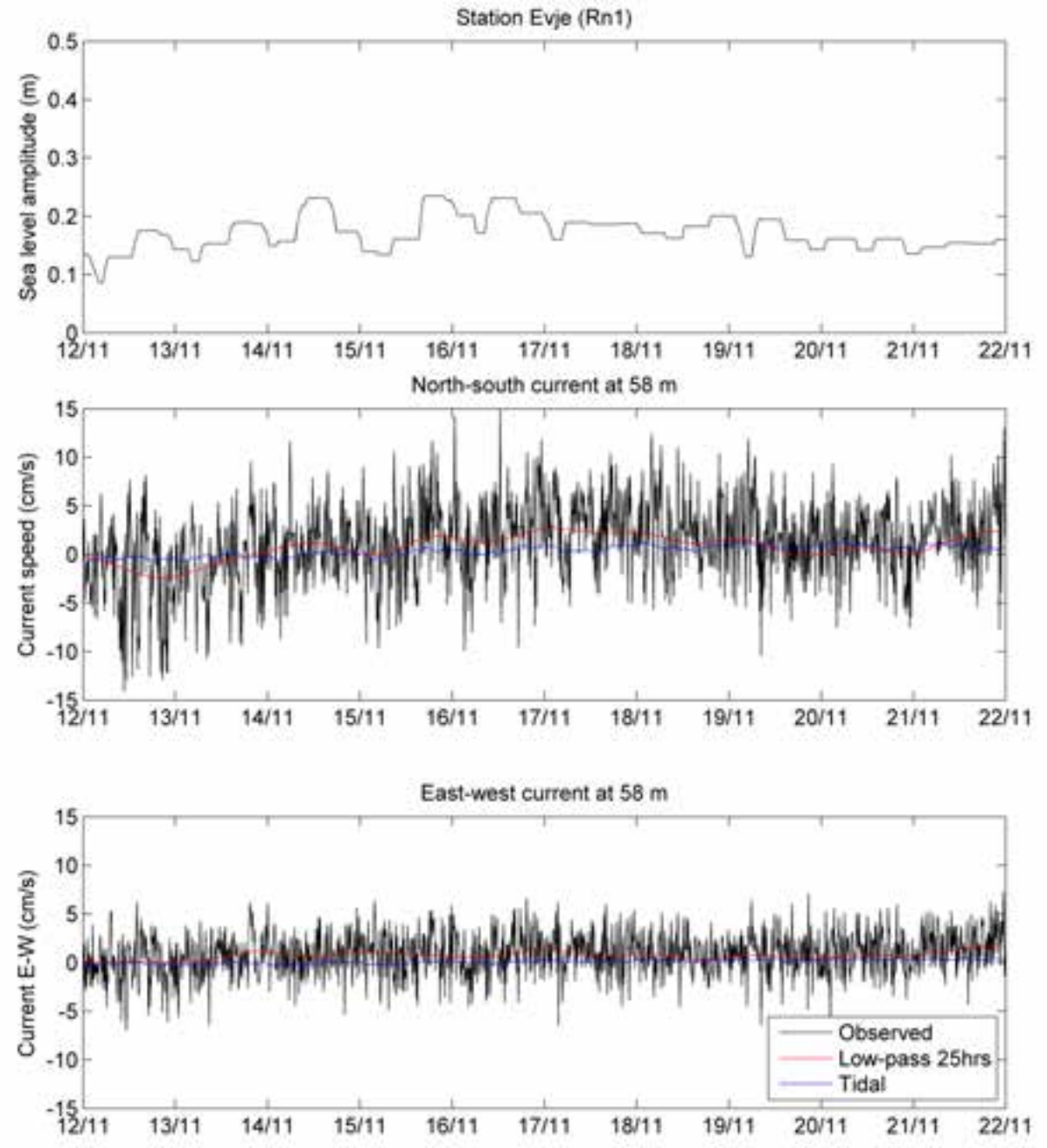

Figure 26. The current 6 m over the bottom at station Evje (middle and lower panel) plotted as a time series together with the sea level amplitude.

4.6 Station Filtvedt (Km1)

At Filtvedt the highest observed current speeds (0.47 m/s) are found at 21 m depth in the north-south direction (**Figure 27** and **Table 8**). Most of the observed variability in the upper layer can be explained by a mean flow and a tidal signal.

The highest observed current speed at the deepest cell of the ADCP measurements was 0.23 m/s (**Figure 28** and **Table 8**). The water depth at this station is approximately 157 m, so this was 11 m over the bottom. Most of the current variability near the bottom can be explained by a mean flow and a tidal signal, but irregular periods of less than 25 hours are also important. The highest currents near the bottom were observed in the north-south direction (**Figure 29**).

Table 8. Maximum current at each depth at station Filtvedt.

Depth (m)	Observed current (m/s)	Tidal current (m/s)	Lowpass 25 hrs current (m/s)
16	0.31	0.10	0.14
21	0.47	0.21	0.22
26	0.36	0.18	0.16
31	0.33	0.17	0.20
36	0.33	0.17	0.17
41	0.30	0.15	0.16
46	0.32	0.15	0.13
51	0.31	0.13	0.15
56	0.31	0.12	0.20
61	0.31	0.10	0.16
66	0.32	0.09	0.16
71	0.30	0.07	0.13
76	0.24	0.07	0.11
81	0.21	0.07	0.12
86	0.22	0.07	0.13
91	0.23	0.09	0.13
96	0.25	0.09	0.12
101	0.25	0.10	0.11
106	0.25	0.10	0.08
111	0.25	0.10	0.06
116	0.25	0.12	0.05
121	0.25	0.12	0.04
126	0.29	0.12	0.04
131	0.29	0.12	0.04
136	0.28	0.11	0.04
141	0.28	0.11	0.05
146	0.23	0.10	0.06

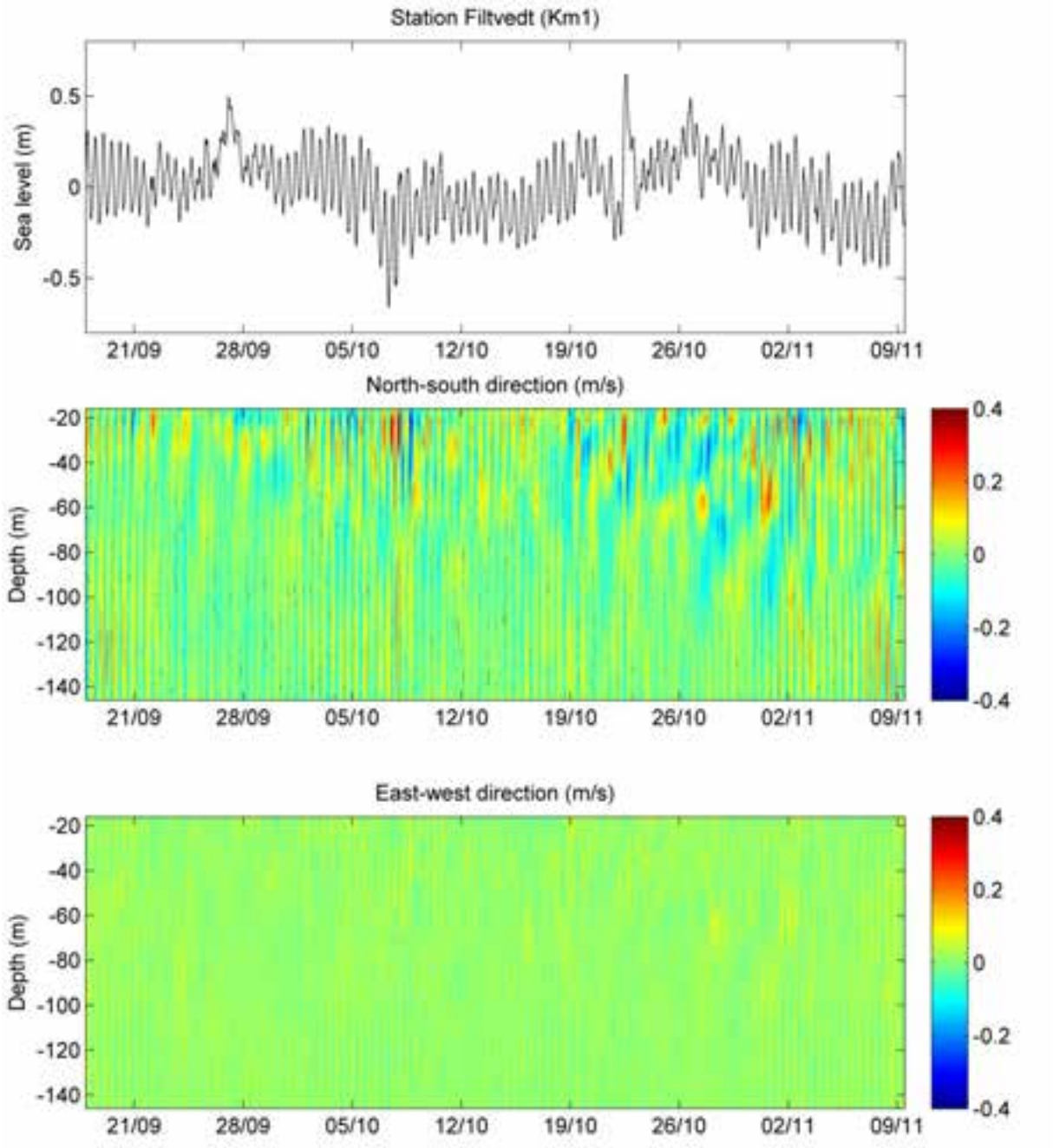

Figure 27. Sea level (upper panel), current in the north-south direction (middle panel) and current in the east-west direction at the station Filtvedt (Km1) from September to November 2014.

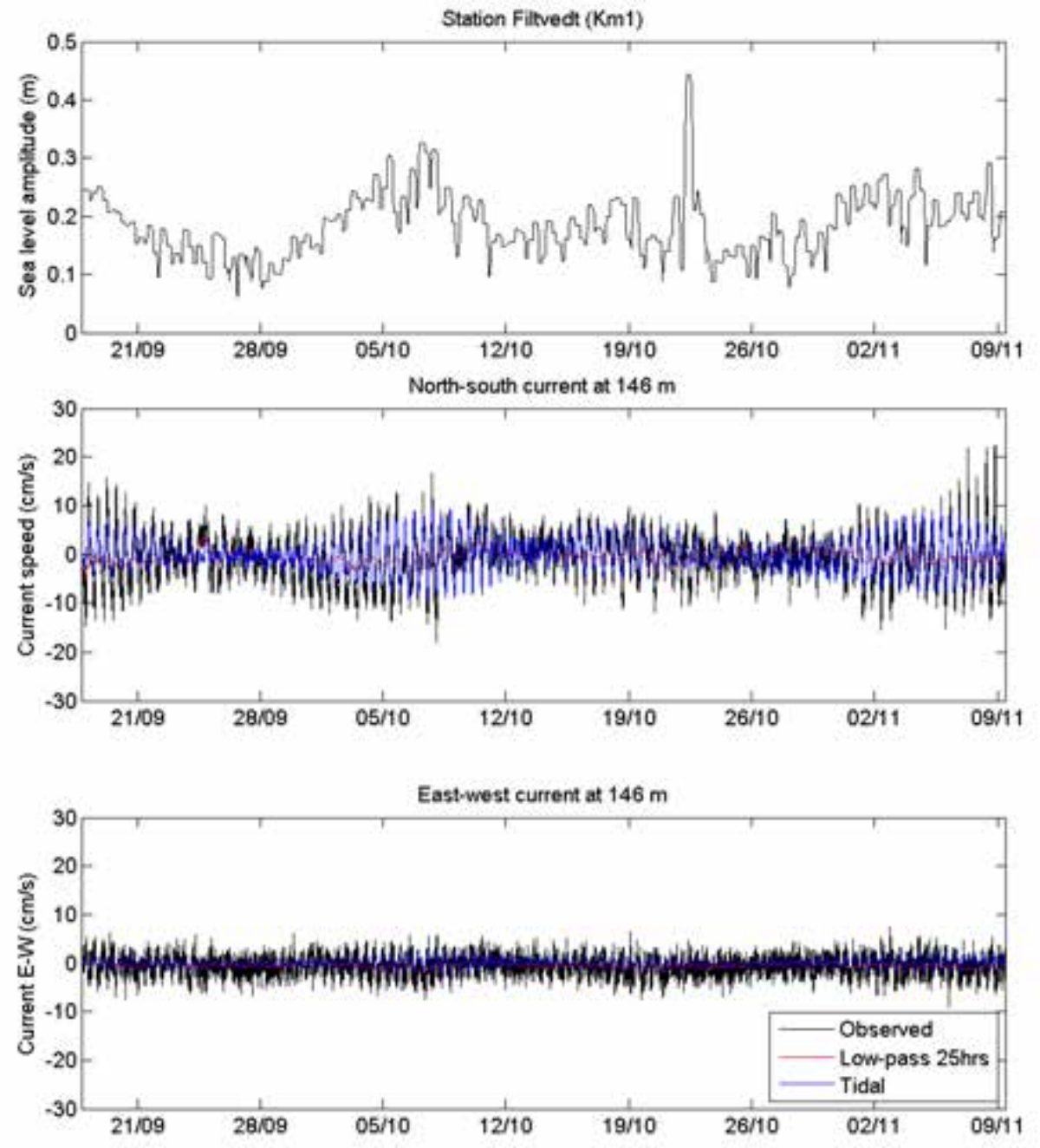

Figure 28. The current 11 m over the bottom at station Småskjær from September to November 2014 (middle and lower panel) plotted as a time series together with the sea level amplitude.

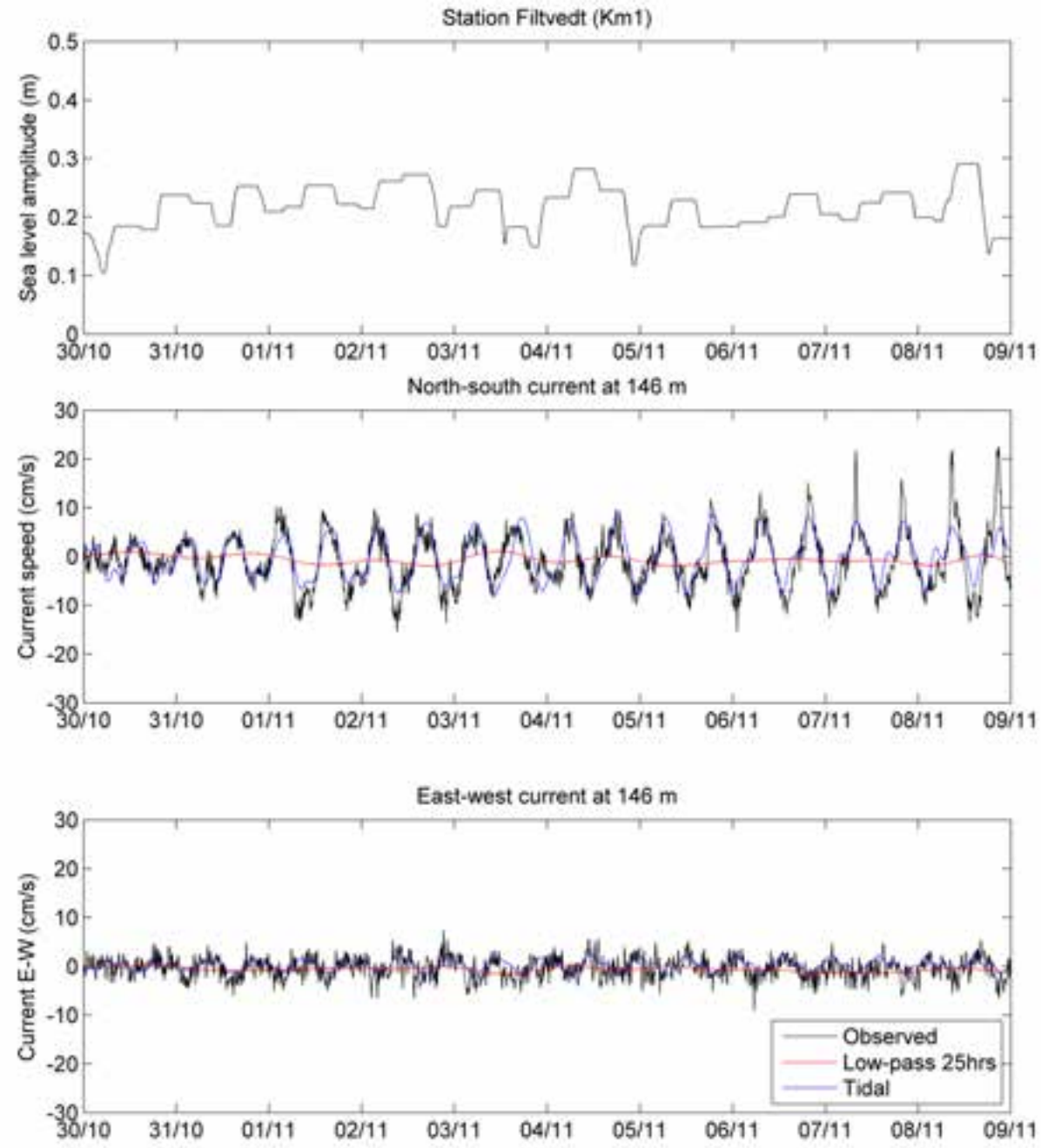

Figure 29. The current 11 m over the bottom at station Filtvedt (middle and lower panel) plotted as a time series together with the sea level amplitude.

4.7 Station Brenntangen (Kn2)

At Brenntangen the highest observed current speeds (0.58 m/s) are found at 7 m depth in the north-south direction (**Figure 30** and **Table 9**). Most of the observed variability in the upper layer can be explained by a mean flow and a tidal signal.

The highest observed current speed at the deepest cell of the ADCP measurements was 0.28 m/s (**Figure 31** and **Table 9**). The water depth at this station is approximately 56 m, so this was 7 m over the bottom. Most of the current variability near the bottom can be explained by a mean flow and a tidal signal, but irregular periods of less than 25 hours are also important. The highest currents near the bottom were observed in the north-south direction (**Figure 32** and **Figure 33**).

Table 9. Maximum current at each depth at station Brenntangen.

Depth (m)	Observed current (m/s)	Tidal current (m/s)	Lowpass 25 hrs current (m/s)
7	0.58	0.23	0.28
10	0.53	0.20	0.19
13	0.44	0.22	0.16
16	0.44	0.21	0.19
19	0.50	0.21	0.22
22	0.43	0.19	0.19
25	0.39	0.17	0.14
28	0.38	0.15	0.14
31	0.38	0.13	0.12
34	0.32	0.12	0.11
37	0.35	0.15	0.11
40	0.30	0.13	0.08
43	0.25	0.12	0.08
46	0.25	0.11	0.07
49	0.28	0.10	0.06

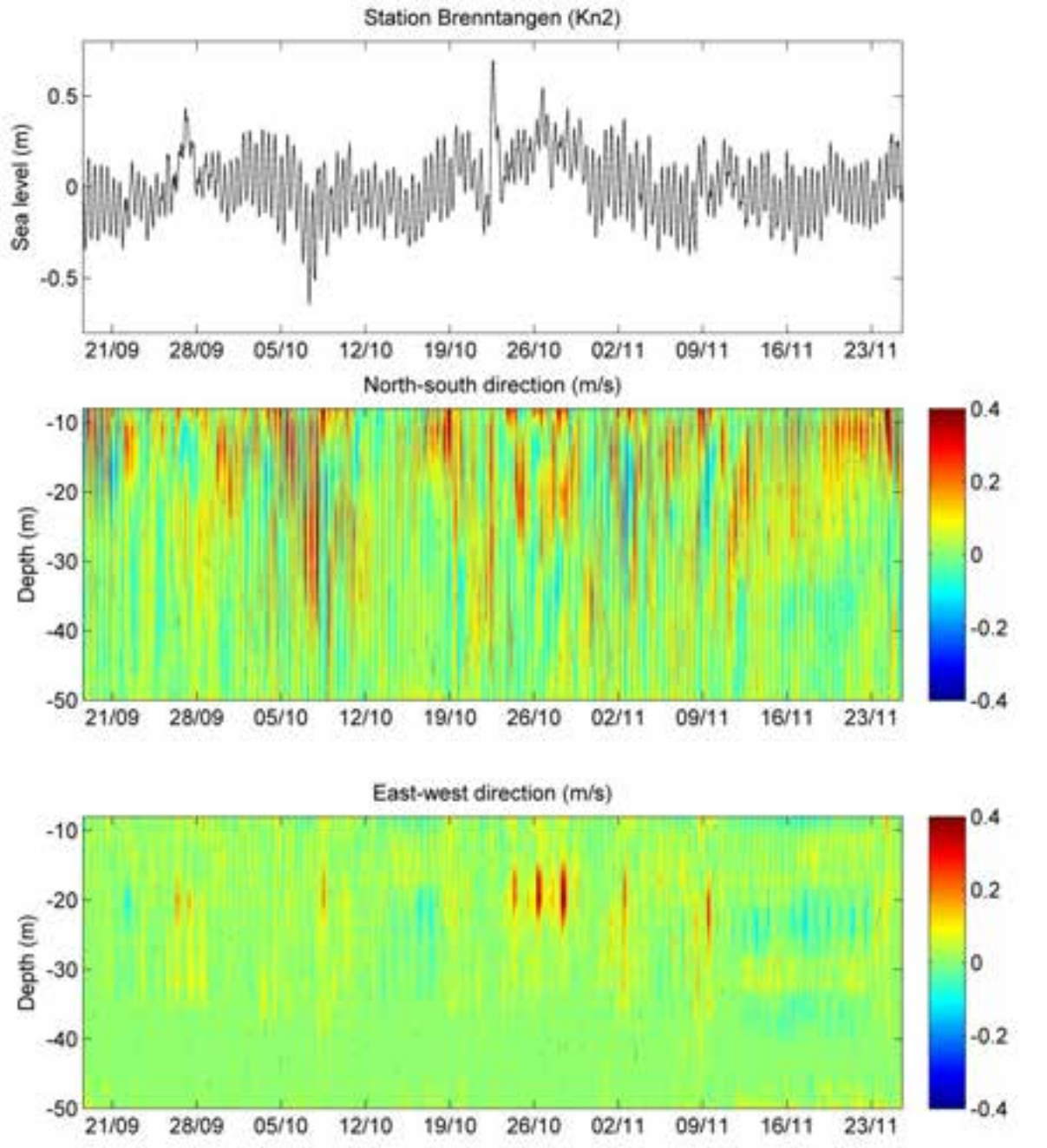

Figure 30. Sea level (upper panel), current in the north-south direction (middle panel) and current in the east-west direction at the station Brenntangen (Kn2) from September to November 2014.

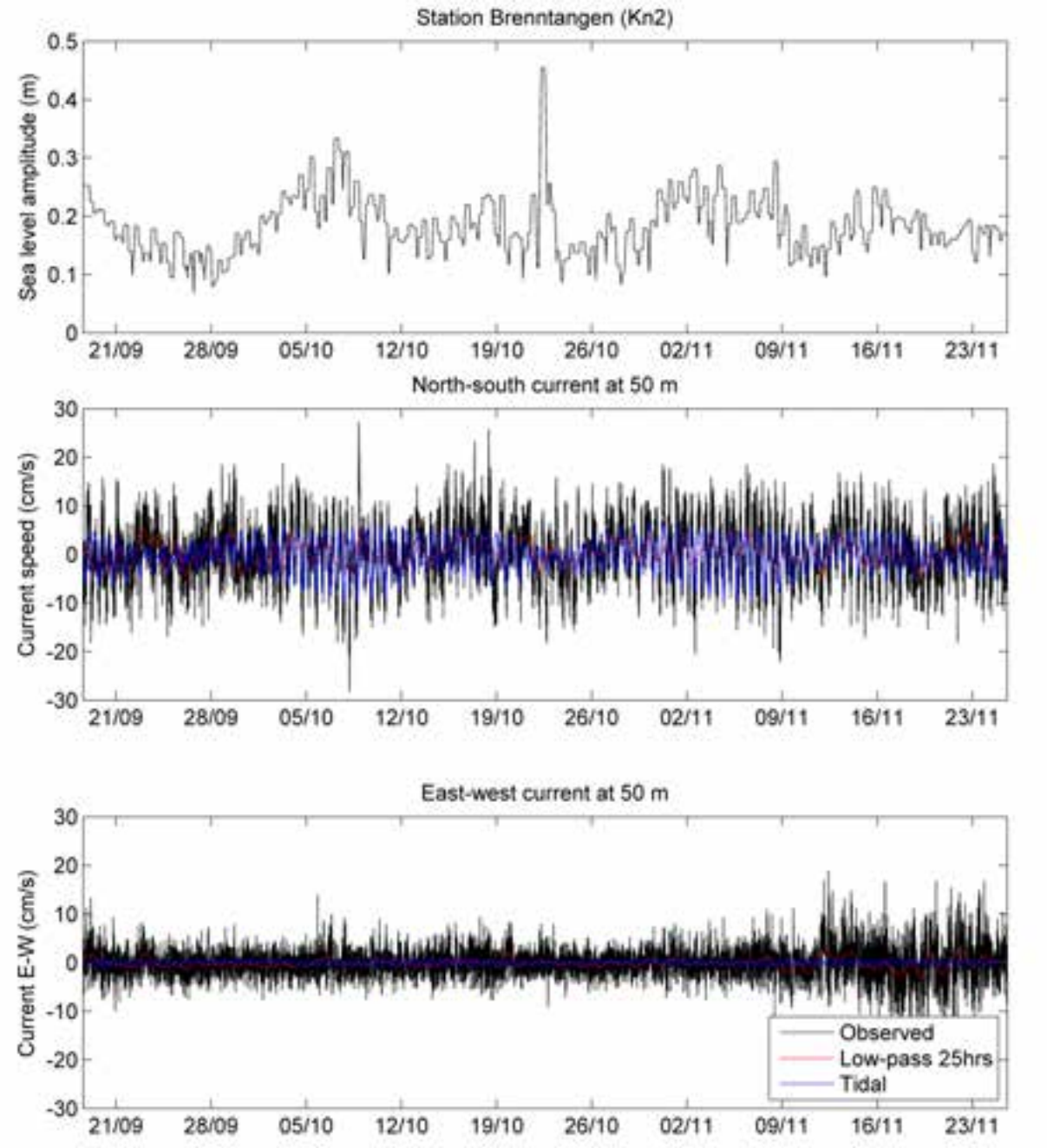

Figure 31. The current 7 m over the bottom at station Brenntangen from September to November 2014 (middle and lower panel) plotted as a time series together with the sea level amplitude.

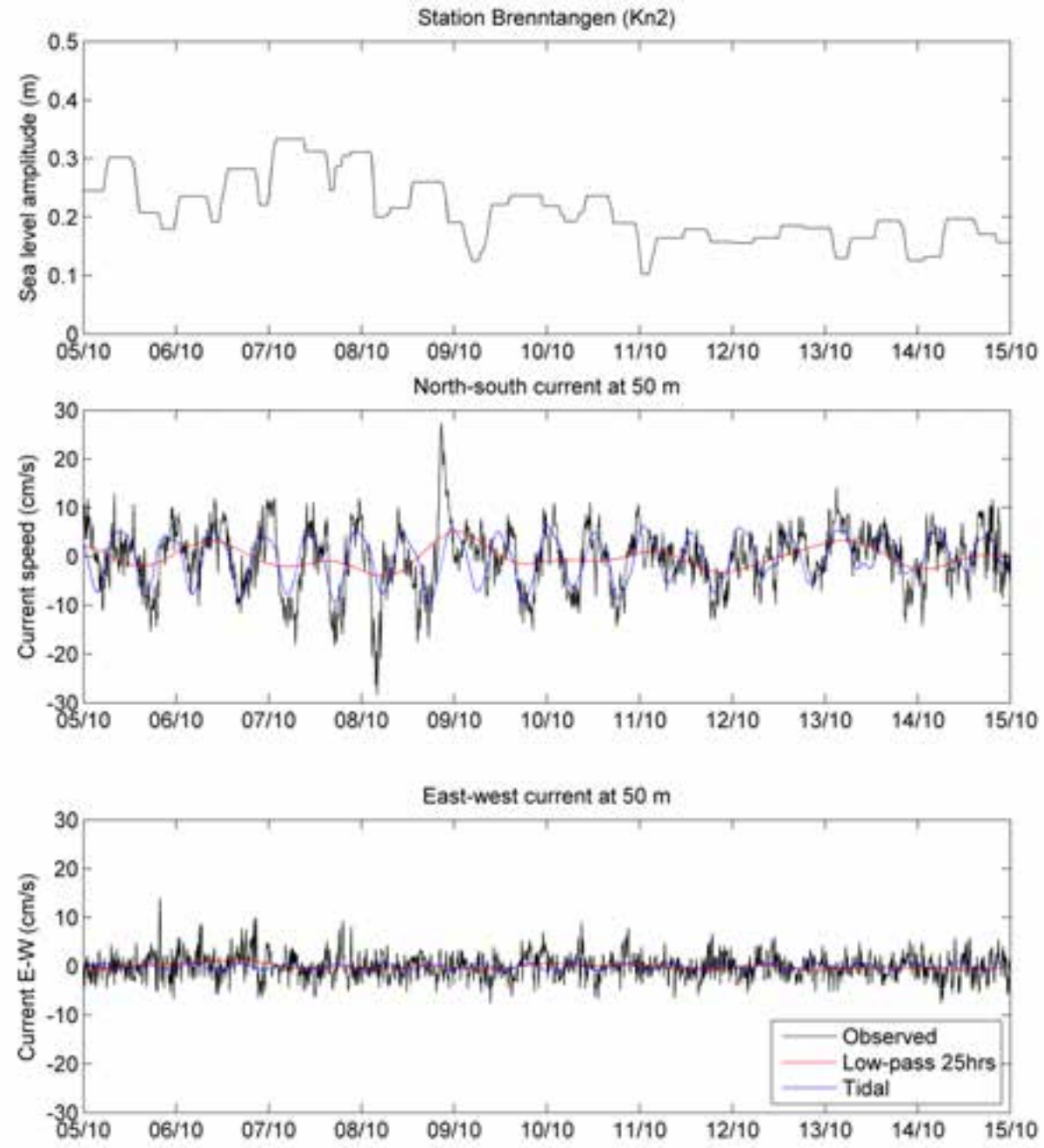

Figure 32. The current 7 m over the bottom at station Brenntangen (middle and lower panel) plotted as a time series together with the sea level amplitude.

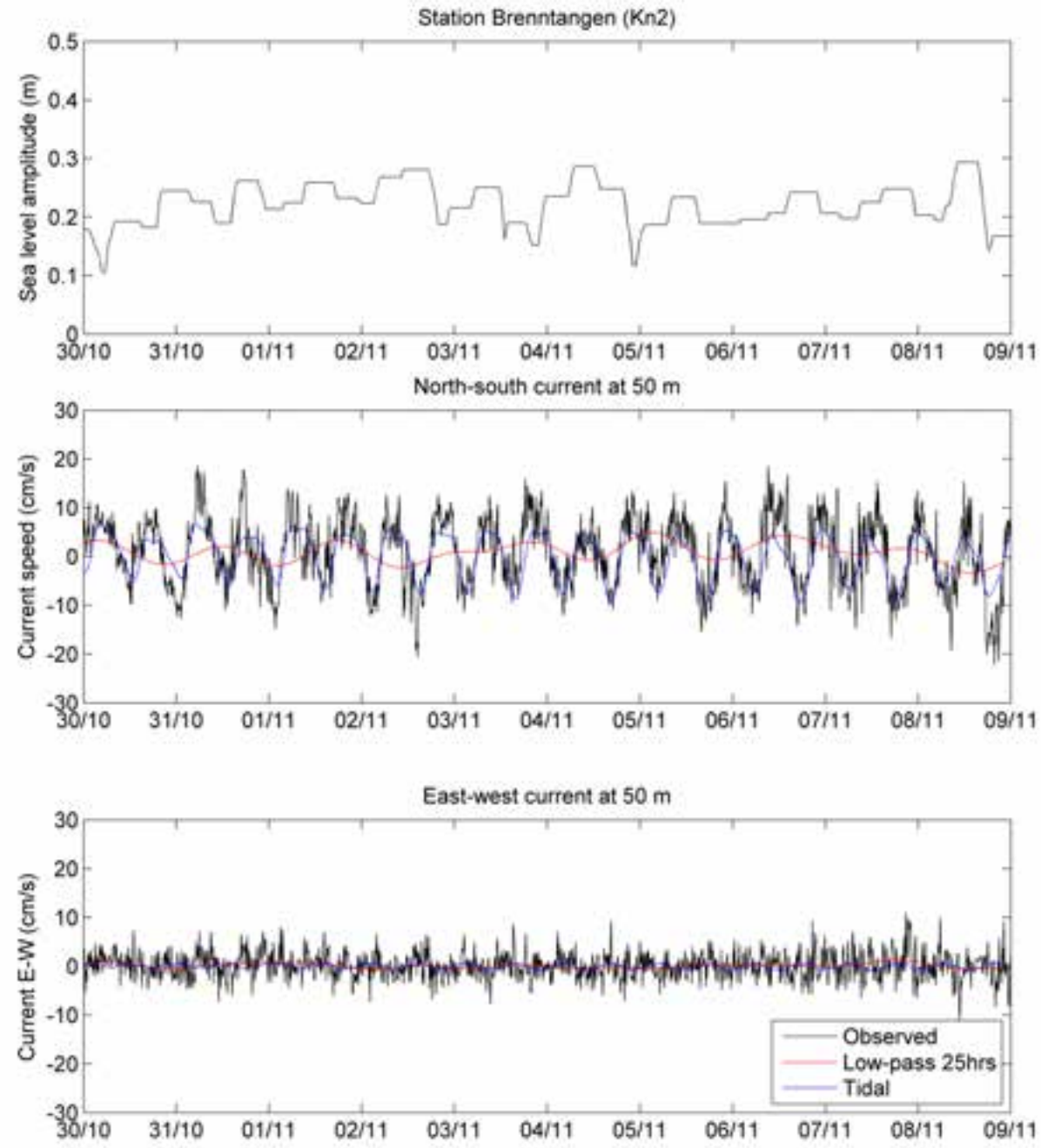

Figure 33. The current 7 m over the bottom at station Brenntangen (middle and lower panel) plotted as a time series together with the sea level amplitude.

4.8 Return period

Figure 34 shows empirical distribution on logarithmic scaled axes and mean excess of the observed velocity magnitude data. The sample mean excess function (MEF) is defined as

$$e_n(u) = \frac{\sum_{i=1}^{n}(X_i - u)}{\sum_{i=1}^{n} 1_{\{X_i > u\}}}. \quad (6)$$

The MEF is the sum of the excesses over the threshold u divided by the number of data points which exceed the threshold u. It is an estimate of the mean excess function, which describes the expected overshoot of a threshold once an exceedance occurs. If the empirical MEF is a positively sloped straight line above a certain threshold u, it is an indication that the data follows the generalized Pareto distribution (GPD)[1] with a positive shape parameter ξ. On the other hand, exponentially distributed data would show a horizontal MEF while short-tailed data would have a negatively sloped line.

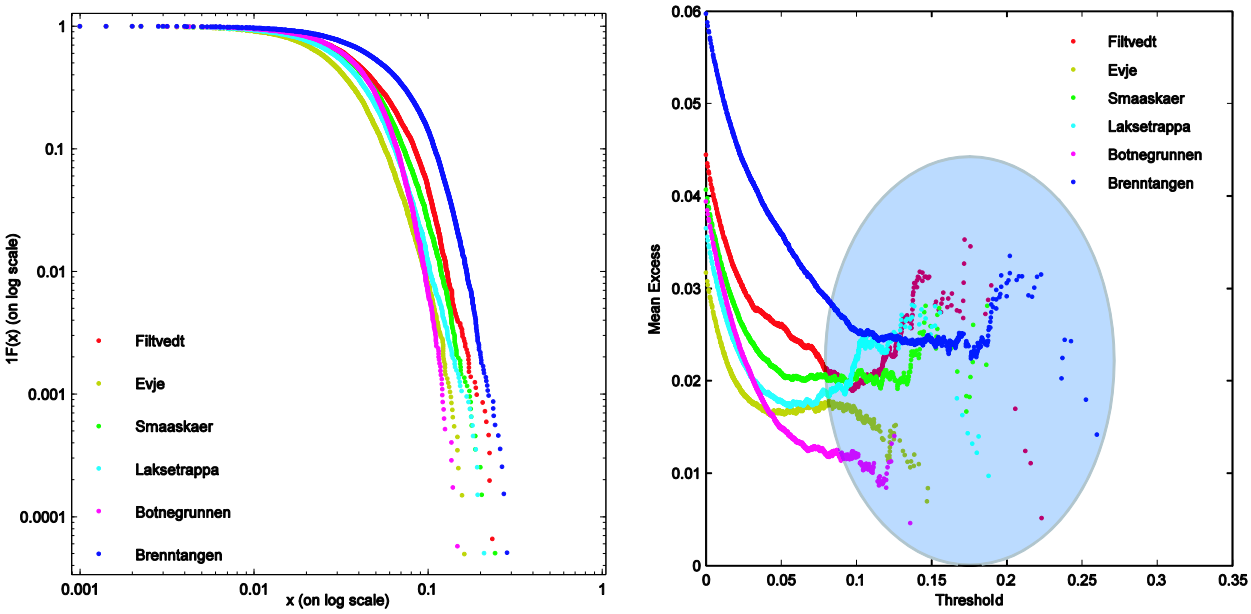

Figure 34. left panel: the normalized empirical distribution function (empirical cdf), right panel: the mean excess graph of the observed current magnitude against threshold value (m/sec).

Notice that a downward exponential trend in the plots up to threshold (~ 0.1) indicates a short-tailed distribution of data. The underlying distribution in the tail is exponential for the area that the slope is approximately zero (shaded in blue). However, a small fraction of the data show upward trend, which indicate a heavy-tail underlying distribution.

In statistics, a quantile-quantile (QQ) plot is a convenient visual tool to examine whether a sample comes from a specific distribution. Specifically, the quantiles of an empirical distribution are plotted against the quantiles of a hypothesized distribution. If the sample comes from the hypothesized distribution, the QQ-plot is linear. In the extreme value theory and applications, the QQ-plot is typically plotted against the exponential distribution (i.e. a distribution with a medium-sized tail) to measure the fat-tailness of a distribution. If the data are from an exponential distribution, the points on the graph would lie along a straight line. If there is a concave presence, this would indicate a fat-tailed distribution, whereas a convex

[1] $$G(x) = \begin{cases} 1 - \left(1 + \xi \frac{x}{\beta}\right)^{-\frac{1}{\xi}} & if\ \xi \neq 0 \\ 1 - e^{-\frac{x}{\beta}} & if\ \xi = 0 \end{cases}$$

departure is an indication of short-tailed distribution. In **Figure 35** it is evident that all of the underlying distributions for the velocity listening have convex departures from the straight line, whereas is an indication of a thin tail.

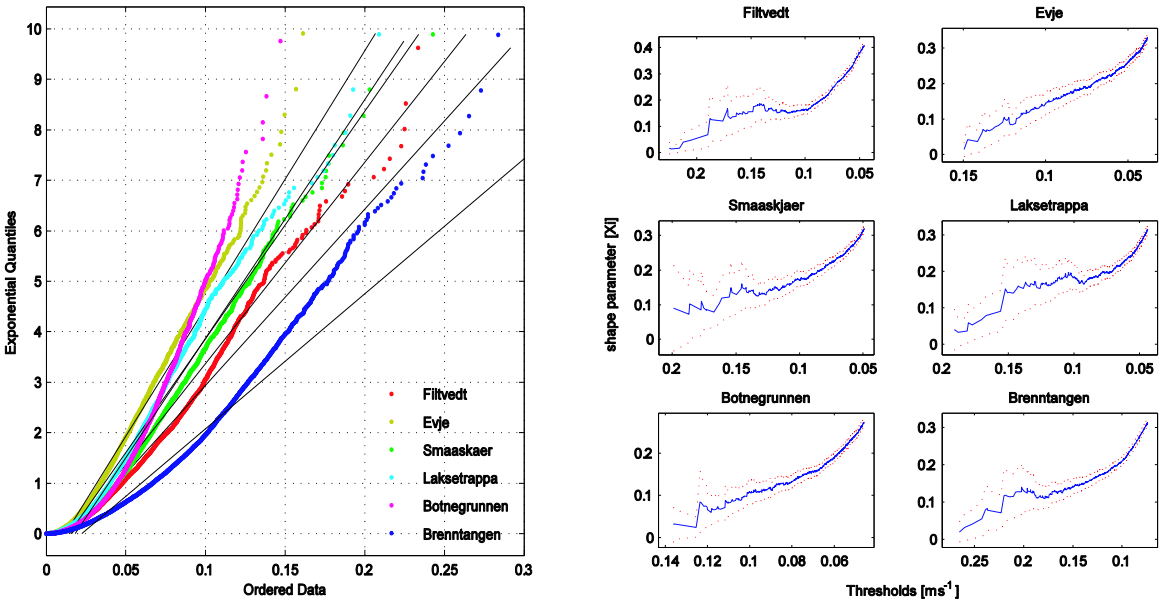

Figure 35. (left panel): QQ-plot of the velocities magnitude data against standard exponential quantiles. Notice that a convex departure from the straight line in the QQ-plot is an indication of a thin tail, right panel: Hill-plot of the data with a 0.95 confidence interval.

The following estimator for ξ is proposed by Hill (1975):

$$\hat{\xi} = \frac{1}{k-1}\sum_{i=1}^{k-1} lnX_{i,N} - lnX_{k,N} \qquad for\ \geq 2, \tag{7}$$

where k is upper order statistics (the number of exceedances), N is the sample size, and $\alpha = 1/\xi$ is the tail index. In **Figure 36** we construct shape parameter plot as a function of the threshold. Then the threshold is selected from the plot where the shape parameter is fairly stable. As it is evident from the graphs, considering a threshold value around 0.15 for the bottom velocities of the stations is justifiable. One exception is Brenntangen station which threshold exceeds to 0.2.

Probability density function (PDF) diagrams for each of the measurements at bottom layer are given in **Figure 37**. According to the PDF diagrams, almost 99% of the bottom velocities are located below 0.15 threshold, and one exception is Brenntangen that shows slightly higher threshold. Red and green curves are Generalized Extreme Value (GEV, see 2.2) and Rayleigh distributions, respectively. Both distributions are fitted to the object data, and apparently, GEV distribution is better representative for the underlying data pattern. Beside the aforementioned distributions, we examined some other well-known distributions in extreme value analysis like as Weibull, Gumbel and Poisson distributions. For all of the stations the best results were achieved using GEV. It worth to mention again that GEV turns to the Frechet, Weibull and Gumbel distributions by taking different shape parameter values. Therefore, Extreme Value (EV) and GEV (see eq. 6) distributions are considered the main underlying data pattern for currents measurements and base for return period calculations (**Figure 37**).

The extreme value distribution is appropriate for modelling the smallest value from a distribution whose tails decay exponentially fast, for example, the normal distribution. It can also model the largest value from a distribution, such as the normal or exponential distributions.

$$f(x|\mu,\beta) = \beta^{-1} e^{(\frac{x-\mu}{\beta})} e^{(-e^{(\frac{x-\mu}{\beta})})}, \quad (8)$$

where $-\infty < x < \infty$, μ is location parameter and β is scale parameter.

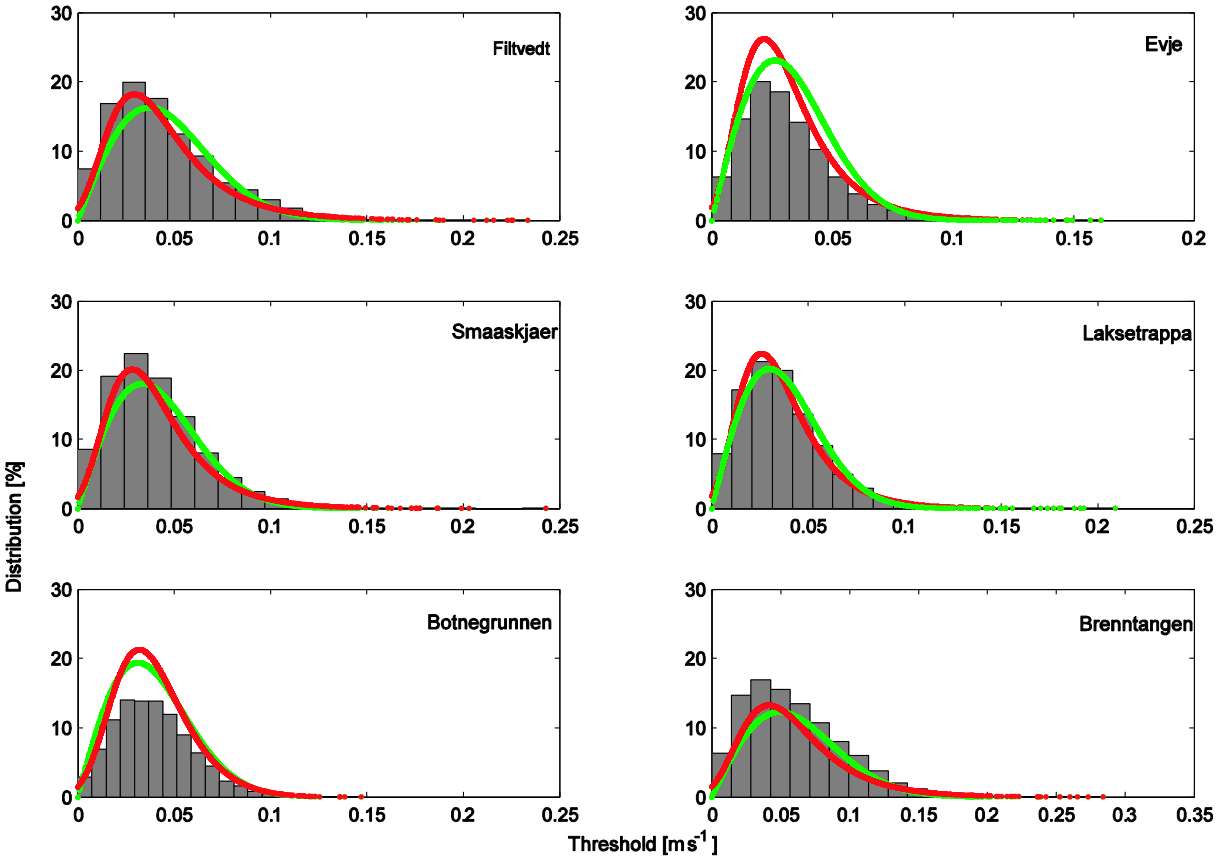

Figure 36. Probability distribution for near bottom current in the stations.

Return periods for 50 years based on EV and GEV distributions are presented in Fig. XX. GEV distribution provides systematically higher extreme current values. However, considering the tail distributions of the measurements, EV distribution provides better results. The maximum 50 years return velocity (approx. 0.46 m/sec) occurs in Brenntangen station and the lowest 50 year return value belongs to Evje station (approx. 0.24 m/sec). Note that all return value calculations were carried out based on the most lower (near to the depth) observation in each station.

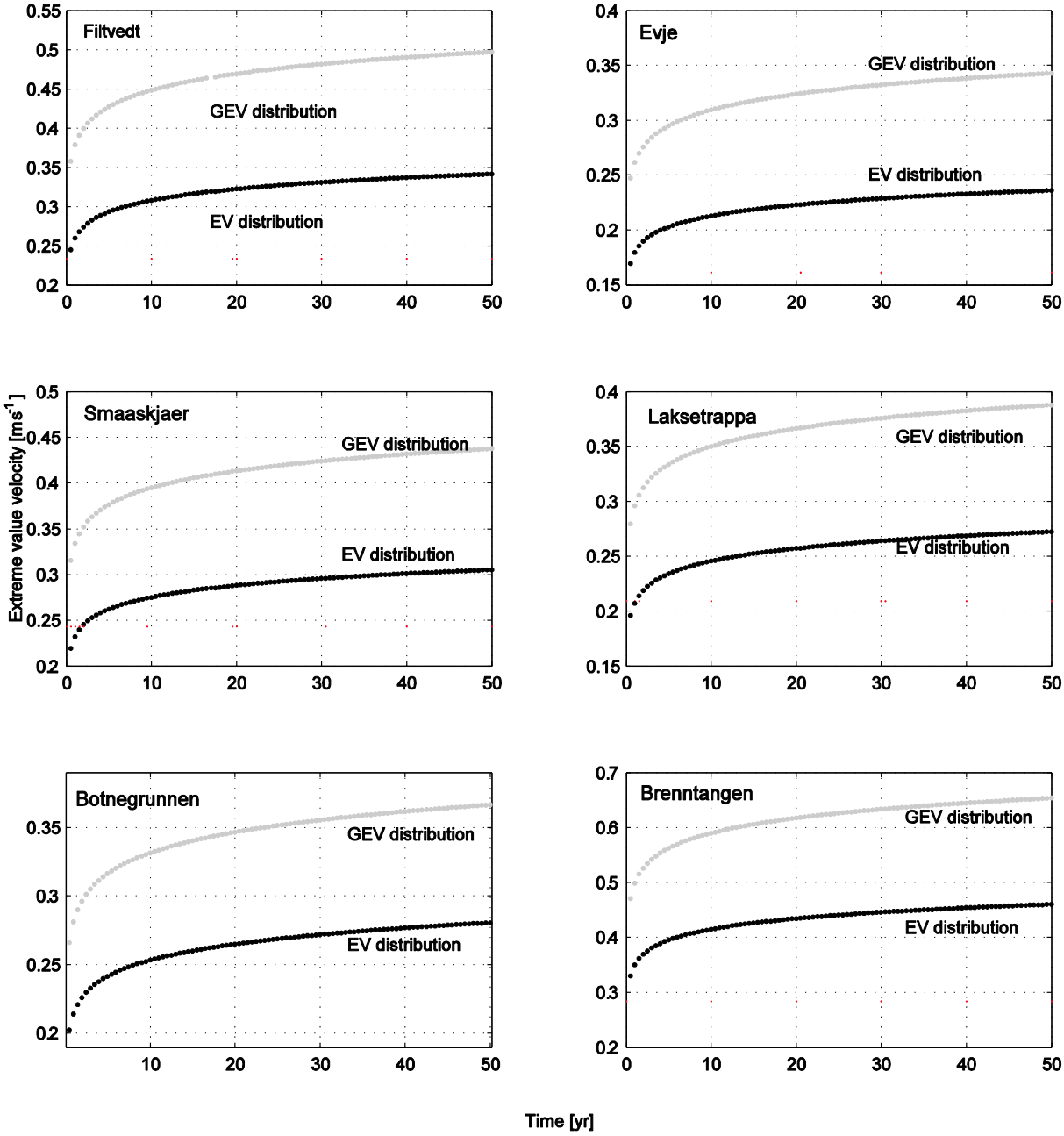

Figure 37. Extreme velocity values for 50 years return period.

5. Summary of results and discussion

The maximum current speeds at the deepest observations at each station are summarized in **Table 10**.

Table 10. Maximum and extreme near bottom currents. For estimates of the extreme currents a Generalized Extreme Value (GEV) distribution is used.

Station	Depth (m)	Meter over the bottom	Observed Current (cm/s)	Tidal current (cm/s)	Mean current (cm/s)	10 year current (cm/s)	10 year current with safety factor (cm/s)	50 year current (cm/s)	50 year current with safety factor (cm/s)
Småskjær	20	3.5	24	2	6	39	59	44	66
Laksetrappa	76	3.0	20	2	5	35	53	39	59
Botnegrunnen	96	13.0	15	1	5	33	50	37	56
Evje	64	6.0	16	1	3	31	47	34	51
Filtvedt	157	11.0	23	10	6	45	68	50	75
Brenntangen	56	7.0	28	10	6	59	89	66	99

An understanding of what cause the flow in a fjord, is useful for an analysis of how strong currents can be. At all the stations oscillations with periods shorter than 25 hours were important, since not all of the observed variability could be explained by a tidal and a mean signal. It is not a trivial task to associate these fast and irregular oscillations with different driving forces directly. The interaction of the mean and tidal flow with the complex bathymetry could be an important factor. It is beyond the scope of this report to explain these irregular oscillations completely, but it is clear from the observations that they are important.

At the four stations south of Bastøy, where the fjord is relatively wide, the tidal signal was almost negligible, and fast and irregular oscillations dominated. At the two stations in the Drøbak Sound where the fjord is relatively narrow, the near bottom current variability could be explained mostly with a tidal signal and a mean flow, but fast and irregular oscillations was also important here. The highest currents were observed at these two stations, implying that the width of the fjord is a significant factor, basically because the tidal current is increased. Another factor that was important for the maximum near bottom currents was the water depth at the stations. In both the two transects across the fjord, it was the shallowest stations that had the highest current velocities. This can be explained by the fact that the horizontal pressure gradient has a tendency to decrease with depth (**Figure 13**).

The highest currents were not directly linked with high sea level amplitudes, but it is likely that high bottom currents are connected with waves originating from flow-topography interaction. Such waves probably have larger amplitudes when the tidal and mean flow is larger, and there could be an indirect link between the highest observed currents and high sea level amplitudes, even though this has not been verified within this project. The largest sea level amplitude during the measurement period was 46 cm. The largest sea level amplitude observed in the period 2000-2013 at the station Oscarsborg, was 68 cm, so it is chosen to use a safety factor of 1.5 that takes into account a possible additive effect of bartropic and baroclinic forcing (see **Table 10**).

Extreme currents are estimated based on statistical probability distributions. Two different extreme value distributions are used, the Extreme Value (EV) and the Generalized Extreme Value (GEV) distribution. The tail of the EV distribution decays exponentially, while the GEV distribution has a more fat tail, and therefor gives higher extreme values. The GEV distribution gave the best description of the observed data, when compared to other possible probability distribution, and is used in **Table 10**. Even though the authors of this report find it unlikely, it cannot be ruled out that a different result of the extreme value analysis with higher extreme values might have been achieved, if an extreme storm surge event, with sea level amplitude of 68 cm, took place during the present measurement campaign. Therefore the result from the extreme value analysis is multiplied with the safety factor of 1.5 in **Table 10**.

6. References

Aas, E. (1994). *De norske farvann.* Institutt for geofysikk, Universitetet i Oslo, 89 pp.

Baalsrud, K., & Magnusson, J. (1990). *Eutrofisituasjonen i Ytre Oslofjord. Hovedrapport.* NIVA-report 2480-1990, 120 pp.

Beirlant, J., Teugels, J., & Vynckier, P. (1996). *Practical analysisi of extreme values.* Leuven: Leuven University Press.

Embrechts, P., Klüppelberg, C., & Mikosch, T. (1997). *Modeling Extreme Events for Insurance and Finance.* Berlin: Springer.

Fisher, R. A., & Tippett, L. H. (1928). Limiting forms of the frequency distribution of the largest or smallest member of a sample. *Proceedings of Cambridge Philoshophical Society, 24*, 180-190.

Hill, B. M. (1975). A simple general approch to inference about the tail of a distribution. *Annals of Statistics, 3*, 1163-1174.

Holm, S. (2014). *Strømmålingsprosjekt 2014, Fartøysoperasjoner.* Statnett 14012 operasjonsplan, rev. 1, 24 pp.

Reiss, R., & Thomas, M. (1997). *Statistical Analysis of Extreme Values.* Basel: Birkhäuser.

Røed, L. P., & Fossum, I. (2004). Mean and eddy motion in the Skagerrak/northern North Sea: insight from a numerical model. *Ocean Dynamics, 54*, 197-220.

Sætre, R. (2007). *The Norwegian Coastal Current - Oceanography and Climate.* Trondheim: Tapir Academic Press.

NIVA: Norway's leading centre of competence in aquatic environments

NIVA provides government, business and the public with a basis for preferred water management through its contracted research, reports and development work. A characteristic of NIVA is its broad scope of professional disciplines and extensive contact network in Norway and abroad. Our solid professionalism, interdisciplinary working methods and holistic approach are key elements that make us an excellent advisor for government and society.

NIVA
Norwegian Institute for Water Research

Gaustadalléen 21 • NO-0349 Oslo, Norway
Telephone: +47 22 18 51 00 • Fax: 22 18 52 00
www.niva.no • post@niva.no